Materials Horizons

ROYAL SOCIETY OF CHEMISTRY

REVIEW

View Article Online
View Journal | View Issue

Cite this: *Mater. Horiz.*, 2023, **10**, 2800

Conductive polymer based hydrogels and their application in wearable sensors: a review

Dong Liu,[a] Chenxi Huyan,[a] Zibi Wang,[a] Zhanhu Guo,[b] Xuehua Zhang,[c] Hamdi Torun,[b] Daniel Mulvihill,[d] Ben Bin Xu*[b] and Fei Chen*[a]

Received 13th January 2023,
Accepted 20th April 2023

DOI: 10.1039/d3mh00056g

rsc.li/materials-horizons

Hydrogels have been attracting increasing attention for application in wearable electronics, due to their intrinsic biomimetic features, highly tunable chemical–physical properties (mechanical, electrical, *etc.*), and excellent biocompatibility. Among many proposed varieties of hydrogels, conductive polymer-based hydrogels (CPHs) have emerged as a promising candidate for future wearable sensor designs, with capability of realizing desired features using different tuning strategies ranging from molecular design (with a low length scale of 10^{-10} m) to a micro-structural configuration (up to a length scale of 10^{-2} m). However, considerable challenges remain to be overcome, such as the limited strain sensing range due to the mechanical strength, the signal loss/instability caused by swelling/deswelling, the significant hysteresis of sensing signals, the de-hydration induced malfunctions, and the surface/interfacial failure during manufacturing/processing. This review aims to offer a targeted scan of recent advancements in CPH based wearable sensor technology, from the establishment of dedicated structure–property relationships in the lab to the advanced manufacturing routes for potential scale-up production. The application of CPHs in wearable sensors is also explored, with suggested new research avenues and prospects for CPHs in the future also included.

1. Introduction

A personalized health monitoring system is considered as one of the pilot units for high-quality healthcare technologies since it can allow faster and effective diagnostics/treatment in a cost-effective manner.[1–6] In this regard, health monitoring systems based on wearable sensors (WSs) have attracted tremendous attention during the past decade, attributed to their facile/conformal interactions with the human body and long-term monitoring capabilities.[7–13] WSs play a critical role in the personalized healthcare sector as an effective transducer to convert the almost imperceptible changes (natural physiological fluctuations) into electrical signals such as impedance,[14–17] potential and current without affecting the user's motions.[18–23] The key to realize the above functions is to develop a soft, biocompatible material that can work conformally on the human body and be compatible with its viscoelastic nature.[24–26]

Hydrogels, a group of soft viscoelastic materials,[27–29] hold huge potential to facilitate versatile structure–property relationships with their designable three-dimensional (3D) crosslinked network and widely available fabrication means ranging from molecular design[30–32] (with a low length scale of 10^{-10} m) to a micro-structural configuration (up to 10^{-2} m),[33–36] which also profoundly affects the physical characteristics of hydrogels[37,38] including the strength, toughness, ductility, corrosion resistance, electrical properties and so on. Another family of functional polymers is conductive polymers (CPs) (*i.e.* polyaniline (PANI), polypyrrole (PPy), and poly(3,4-ethylene dioxythiophene): poly(styrene sulfonate) (PEDOT:PSS)) representing a class of polymers that have a delocalized π system backbone enabling charge transfer along the polymeric chains, exhibiting electrical conductivity.[39–45]

CPs are kinds of organic materials with specific electrical and electrochemical performances, combining the advantages of carbon/metals as good conductors and polymers as low-cost and flexible materials. The unique combined properties of CPs have attracted great interest for various biomedical applications such as biosensors, neural probes, drug-delivery devices, bio-actuators and tissue-engineering scaffolds.[46] PANI, PPy and PEDOT are some of the most widely used CPs, and have been considered as the alternatives to carbonaceous and metallic nanofillers for developing ECHs because of some of their special and unique properties such as high electrical conductivity,

[a] *School of Chemical Engineering and Technology, Xi'an Jiaotong University, Xi'an, 710049, P. R. China. E-mail: feichen@xjtu.edu.cn*
[b] *Mechanical and Construction Engineering, Faculty of Engineering and Environment, Northumbria University, Newcastle upon Tyne, NE1 8ST, UK. E-mail: ben.xu@northumbria.ac.uk*
[c] *Department of Chemical and Materials Engineering, University of Alberta, T6G 1H9, Edmonton, Alberta, Canada*
[d] *Materials and Manufacturing Research Group, James Watt School of Engineering, University of Glasgow, Glasgow G12 8QQ, UK*

Table 1 Properties of common CPs

Polymer	Properties	Limitations
PANI 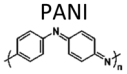	Easy synthesis method High stability Low cost Large specific surface area High electrical conductivity	Non-biodegradable, Lack of flexibility Limited solubility Low processability Poor cycling stability
PPy 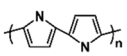	Easy to synthesis Stable in an oxidized form Non–toxic	Brittle Insoluble Non-transparent
PEDOT 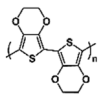	Environmentally stable Electrochemically stable Tunable conductivity Non-toxic	Poor solubility Limited flexibility Hard to process.

electrical properties, reversible doping/dedoping process, preparation simplicity, controllable chemical and electrochemical properties and environmental friendliness. CPs are a class of conjugated π polymers, possessing typical p-conjugated structures which enable electrons to stay and transfer in their backbones.[47] The conductive pathway is constructed by the freely moving delocalized π-electrons, thus providing an electrical route for mobile charge carries,[48] leading to controllable conductivity[49] (Table 1). Therefore, CPs are frequently utilized as electrode materials for stimulation and recording, owing to their unique capability of chemical surface modification with physiologically active species to improve the biocompatibility and functionality. However, their application in WSs is limited because CPs are brittle and difficult to handle. Combining CPs with another polymer can combine the useful properties of both materials, in order to overcome the drawbacks of CPs and make full use of their advantages. Using an appropriate method to construct CPHs can provide the increased solubility and better mechanical properties of CPHs, necessary for various WSs without significant compromise of their unique properties. Details are discussed in later sections.

Conductive polymer-based hydrogels (CPHs) can be synthesized by employing CPs as scaffolds for constructing continuous conductive networks in a hydrogel, facilitating the transport and diffusion of electrons and charges.[48–50] The resulting CPHs have been an effective building block for WSs, owing to their excellent conductivity (up to 10^3 mS m^{-1}), good biocompatibility, easy processing, environmentally friendly properties and cost-effectiveness.[51–53] The CPs are the conductive unit of the bulk hydrogels, while the electrical conductivity in CPHs is entirely provided by their conductive networks formed with CPs. Enhancing the content of CPs in CPHs could efficiently improve the bulk conductivity of CPHs, owing to that the isolated electronic transfer pathway gradually evolved into a 3D conductive network, resulting in higher conductivity. Then, the CPs come into contact with each other to construct a whole conductive network for electron transporting with relatively low resistance. At this point, the conductivity of the bulk hydrogel depends on the inherent conductivity of the CPs. For example, Wang *et al.*[54] demonstrated that the conductivity of optimized PANI based CPHs could achieve 8.24 ± 0.57 S m^{-1}, which is close to that of the pure PANI hydrogel.[55] CPHs have also been utilized for flexible bioelectronics to improve the interface between biological and synthetic systems as well as the performance of medical devices.[56–65] Compared to a blend of metallic/carbon particles that are island-type distributed in the polymer matrix, CP chains are able to construct an ideal 3D interconnected conducting network. The interconnected conductive paths were suitable for accomplishing efficient tunnelling current, resulting in high electro-conductivity.[66,67] However, there still remain technical obstacles: CPs have low water solubility, and hydrophobic CPs are easy to aggregate in hydrogels if there is no chemical bond between CPs and hydrophilic chains. As a result, (1) the continuous conductive network in the CPHs is destroyed, significantly decreasing their conductivity, and (2) the aggregated CPs in the hydrogel tend to be stress concentration points when the CPHs are subjected to an external force, decreasing their capacity to withstand significant stress.

Considering these issues, continuous efforts have been devoted to improve the conductivity and mechanical performance of CPHs for high performance WSs, by building in a precise and robust mechanical–electrical sensing response,[68,69] towards a wide range of applications.[70–72] This review focuses on the construction of structure–property relationships of CPHs for the temperature or/and mechanical sensing (Fig. 1). We start by reviewing the development of the novel network structure of CPHs, the associated strategies to realise these CPHs, and the various fabrication/integration approaches for CPH-based WSs. Then, we discuss the state-of-the-art in CPH-based WSs covering the sensing principles and the underlying mechanisms. A summary and outlook are then provided at the end with exploration of the future design of CPH-based WS devices.

2. Fabrication of CPHs

CPs are hard to fabricate due to the aromatic structure and the intermolecular hydrogen bond between the amine and imine

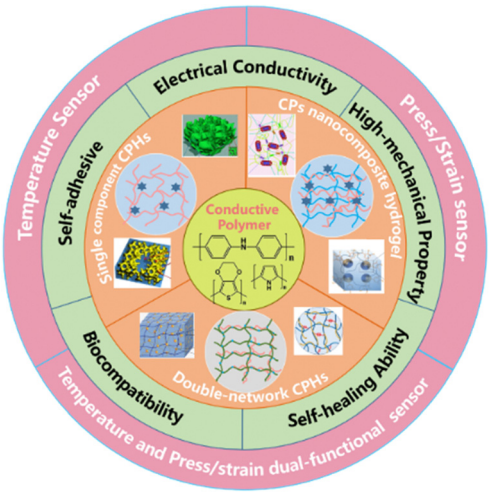

Fig. 1 Schematic illustration of three categories of network structures of CPHs and their properties and applications being reviewed.

groups, resulting in insolubility in most solvents.[73–75] The insolubility leads to the inhomogeneous distribution of CPs in hydrogel networks, eventually compromises the mechanical and electrical properties. The homogeneous distribution of polymer chains to generate a continuous network is crucial to fabricate WSs with high sensitivity. According to the percolation threshold theory, the uniformly distributed electronic CP chains in CPHs are in contact with each other when the concentration of the CPs increased to their percolation threshold, building a continuous 3D conductive network. Under this condition, the interior conductive network exceeded slightly under faint deformation, leading to sharply fluctuated conductivity. The increase in $\Delta R/R_0$ (for resistive-type strain sensors, GF = $(\Delta R/R_0)/\varepsilon$, where $\Delta R/R_0$ is the relative resistance change and ε is the strain) is due to the deformation and disconnection of the internal conductive network within the film, corresponding to the high sensitivity.[76] Otherwise, the island distributed CPs cannot construct the continuous conductive network in CPHs, and their $\Delta R/R_0$ are insensitive to the external stimuli. Different synthetic approaches have been developed to address these concerns with processability by incorporating hydrophilic substituents and copolymerizing aniline with other monomers to generate soluble copolymers – this will be reviewed in the following section.

2.1. Synthetic processing of CPHs

The most effective way to synthesize the CPH network is the copolymerisation of CP monomers with non-conductive polymers. However, the copolymerized CPs are non-elastic with limited stimuli-responsiveness, due to the constrained mobility of chains caused by strong interactions between fillers and the polymer matrix.[50] To realize a continuous conducting network in CPHs, non-conductive polymers and CP precursors are combined and polymerized either in a two-step procedure (Fig. 2a and b) or self-assembly in one step (Fig. 2c) to merge the CP into an insulating hydrophilic polymer matrix. The hydrophilic polymer acts as either a fragment of the main copolymer chains or a cross-linking unit to bridge CPs.

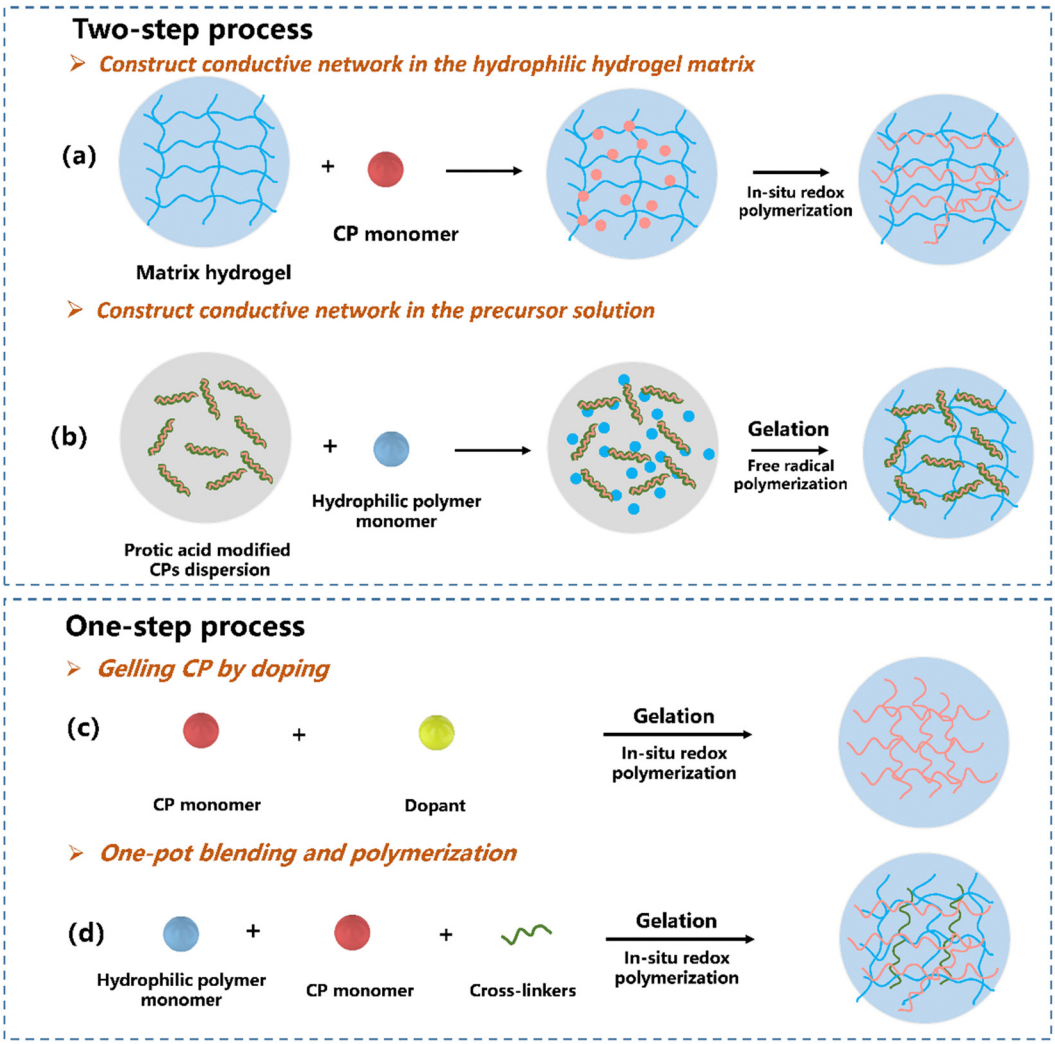

Fig. 2 Schematic illustration of common synthetic approaches to prepare CPHs. (a) Construction of a conductive network in the hydrophilic hydrogel matrix. (b) Construction of a conductive network in the precursor solution. (c) One-step gelling CPs by doping. (d) One-pot blending and polymerization.

2.1.1. Two-step synthesis. The two-step synthesis of CPHs has two routes to achieve a conductive network: (1) achieving the homogeneous distribution of the polymer conductive networks in the hydrophilic hydrogel matrix (Fig. 2a). In this route, non-conductive hydrophilic polymer hydrogels are first formed by UV curing or free radical polymerization, such as poly(*n*-isopropyl acrylamide) (PNIAM), polyacrylic acid (PAA), and polyacrylamide (PAAM or PAM).[77–79] Then, the CPs are introduced into the hydrogel matrix to initialize the electron transfer pathways by absorbing the CP monomers into the hydrophilic hydrogel matrix, followed by the *in situ* redox polymerization to create a conductive network of CPHs.[80–82] (2) Constructing a conductive network and then gelling (Fig. 2b). The CPs are treated with amphiphilic molecules and/or surfactants to enhance the water solubility and mixed with other monomers uniformly. Then, free radical gelation is performed to achieve CPHs.

Constructing the conductive network in the hydrophilic hydrogel matrix. This is the most common route to build CPHs with a continuously conductive network. The hydrophilic hydrogel is soaked in a conductive monomer solution to allow the monomer to sufficiently diffuse inside the porous structure of the hydrogel and then the favoured network is generated by oxidative polymerizing of CPs.[86,87] Lu's group[83] designed a tough and conductive PPy-PAM/chitosan (PPy-PAM/CS) hydrogel by employing the CS framework as molecular templates to control the *in situ* formation of PPy nanorods within the hydrogel networks (Fig. 3a). The hydrophobic PPy nanorods were uniformly dispersed and merged with the hydrophilic polymer phase in the PPy-PAM/CS hydrogel, resulting in outstanding conductivity, mechanical characteristics, and biocompatibility.

Constructing a conductive network in the precursor solution. In this route, the morphology and physical/chemical properties of CPs can be manipulated using doping principles during the synthesis.[88,89] Our group developed a strand entangled supramolecular PANI/PAA hydrogel *via* a "doping then gelling" strategy[84] (Fig. 3b). The PANI nanorod was first doped with

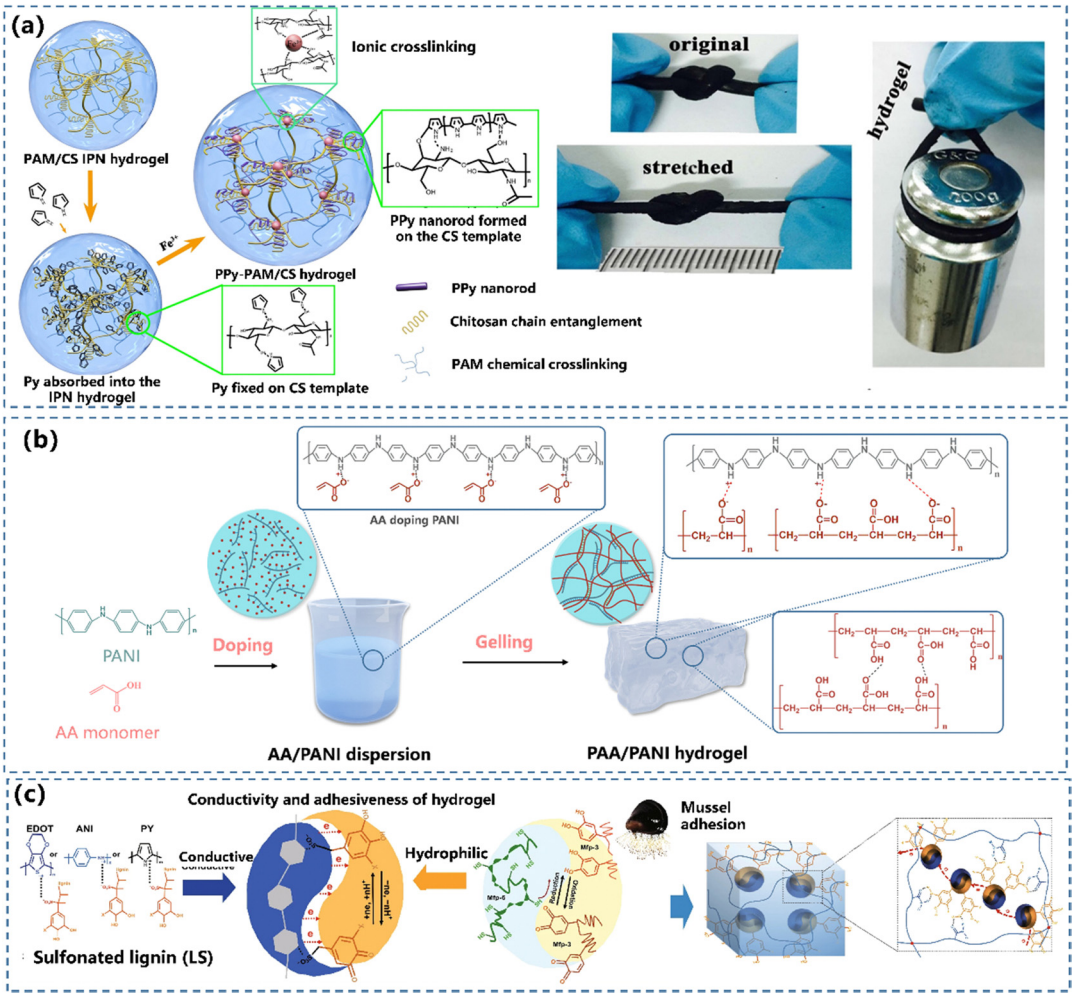

Fig. 3 Construction of a conductive network in the hydrophilic hydrogel matrix: the preparation and schematic illustration of the structure of the (a) PPy-PAM/CS hydrogel. Reprinted from ref. 83 with permission. Copyright 2018 American Chemical Society. (b) The process of the "doping then gelling" strategy to prepare the PAA/PANI gel. Reprinted from ref. 84 with permission. Copyright 2022 John Wiley and Sons. (c) Preparation of hydrophilic and redox-active CP/LS NP hydrogels. Reprinted from ref. 85 with permission. Copyright 2020 Springer Nature.

an acrylic acid (AA) monomer, while the AA doped PANI nanorod possessed not only favourable dispersiveness but also enhanced conductivity. Lu *et al.*[85] developed universal technology to achieve CPHs by doping various CPs (PANI, PPy and PEDOT) with catechol/quinone contained sulfonated lignin, which significantly improved the water solubility of CPs (Fig. 3c). The obtained CPHs possessed high conductivity with a well-constructed electric path, and even a long-term adhesiveness.

The down-sizing of CP particles can also improve the dispersion of CPs into water. Yu's group[90] combined PANI nanoparticles with the poly(poly(ethylene glycol) methacrylate-*co*-AA) (P(PEG-*co*-AA)) network to fabricate CPH-based WSs with high stretchability, ultra-softness, excellent conductivity, and good self-healing ability. Benefiting from the homogeneous dispersion of nano-sized PANI and dynamically electrostatic interactions/hydrogen bonds between PANI and the P(PEG-*co*-AA) scaffold, the obtained CPHs exhibited an excellent stretchability, a low modulus, and a fast self-healing performance. In addition, the subsequent demonstration of CPH-based WSs show a unique strain detection, with a large range of linearity and outstanding anti-fatigue feature.

2.1.2. One-step process

Gelling CPs by doping. One-step gelling of CPs by doping is conducted by directly cross-linking CP chains without an additional insulating hydrophilic polymer matrix (Fig. 2c), feasible for constructing CPHs by introducing other cross-linkers with multi-functional groups such as PA,[55] copper phthalocyanine-3,4,4,4′-tetrasulfonic acid tetrasodium salt (CuPcTs)[91] and amino trimethylene phosphonic acid.[92] Owing to the six anionic phosphate groups, Bao[55] have fabricated PANI based 3D porous CPHs by using PA as both the dopant and the gelator to interact with PANI chains. Moreover, plant-derived polyphenol tannic acid that contains multi-phenolic hydroxyl groups can also act as the dopant and the crosslinker for the conductive PPy hydrogel by constructing abundant intermolecular interactions.[93] As a result, a soft, highly conductive, biocompatible CPH was developed.

One-pot blending and polymerization. CPHs can be fabricated by one-pot blending of conducting precursors and hydrophilic precursors, followed by *in situ* polymerization for gelation[94–97] (Fig. 2d). Among notable examples, Moussa *et al.* demonstrated a universal method to achieve CPHs with a wide range of CPs including PANI, PPy and PEDOT,[98] while Zhao *et al.*[99] directly mixed PANI and crosslinked PVA to acquire stretchable CPHs *via* an ice-templated, low-temperature polymerization. The resulted CPHs exhibited enhanced mechanical, electrical and electrochemical properties, with capability to monitor human motions at both large and small strains in real time. With a self-assembly process, the solution-processing issue is not a problem for CPs. PEDOT:PSS consisting of both positively charged conjugated PEDOT and negatively charged saturated PSS can be processed using this route.[100,101] Bao *et al.* developed PEDOT:PSS hydrogels by using ionic liquid 4-(3-butyl-1-imidazolio)-1-butanesulfonic acid triflate to increase the ionic strength of PEDOT:PSS solutions, yielding a remarkable enhancement in conductivity. Wu *et al.*[94] synthesized highly stretchable supramolecular CPHs by doping poly(*N*-acryloyl glycinamide-*co*-2-acrylamide-2-methyl propane sulfonic) (PNAGA–PAMPS) with PEDOT:PSS. The PNAGA-PAMPS hydrogels exhibited excellent mechanical properties such as 1700% elongation at the breaking point, and a giant capacity due to the addition of PEDOT:PSS.

Notably, blending PEDOT:PSS with other non-conductive polymers always suffers from compromised mechanical and/or electrical properties. Zhao' team[39] reported interesting pure PEDOT:PSS by interconnecting networks of PEDOT:PSS nanofibrils. Different from the commonly used method, they used a simple method by mixing volatile organic solvents with aqueous PEDOT:PSS solutions followed by controlled dry-annealing and rehydration, constructing high performance CPHs with controllable electrical conductivity, superior mechanical properties, and tunable isotropic/anisotropic swelling in wet physiological environments.

2.2. Manufacturing process of CPHs

Subjected to the synthetic route of CPHs, it can also be manufactured through different processes such as casting/molding and 3D printing to achieve certain geometries. The manufacturing process can strongly influence the morphology of conductive networks and hence greatly affect their mechanical properties.[102,103] In the following section, we will review these two popular manufacturing processes.

2.2.1. Casting and molding. The casting and molding process is a conventional approach to create CPHs with desirable morphology with advantages such as simplicity, high throughput and low cost.[104–107] In this method, a hydrogel pre-solution is poured into a shaped mold, followed by polymerization which can be triggered by a range of stimulus, *i.e.* light, chemicals, or heat for gelling.[108–110] This robust method has been widely used to fabricate simple and planar shaped two-dimensional (2D) or 3D structures for CPHs.[111,112] Zhou's group[113] reported a hybrid PVA/PANI hydrogel with a fully physical cross-linked binary network acting as an electrode of the pressure sensors. Based on the molding and casting process, hydrogels with reliefs were forged. The specific reliefs on the surface of 2D PVA/PANI effectively enhance the gauge factor of WSs, resulting in a high GF of 7.70 kPa^{-1} and a sensing range of 0–7.4 kPa.

2.2.2. Additive manufacturing (3D printing). 3D printing is attractive as it can generate 3D structures in a layer-by-layer fashion through a computer aided design (CAD).[114,115] 3D printing technologies with appropriate "biocompatible inks" are potentially able to fabricate WSs with precise control. Extrusion-based and light curing-based 3D printing techniques have been demonstrated to print 3D structures by using DN hydrogels to achieve high stretchability, good toughness, and unique biocompatibility.[116,117] Different from the free-standing 3D CPH structures that can be engineered by relocating the pre-printed designs on substrates through tiny nozzles, the 3D printing of CPHs can accomplish structures with complex and reproducible geometries with a resolution of a few hundred micrometers, which often relies on the shear thinning behaviour

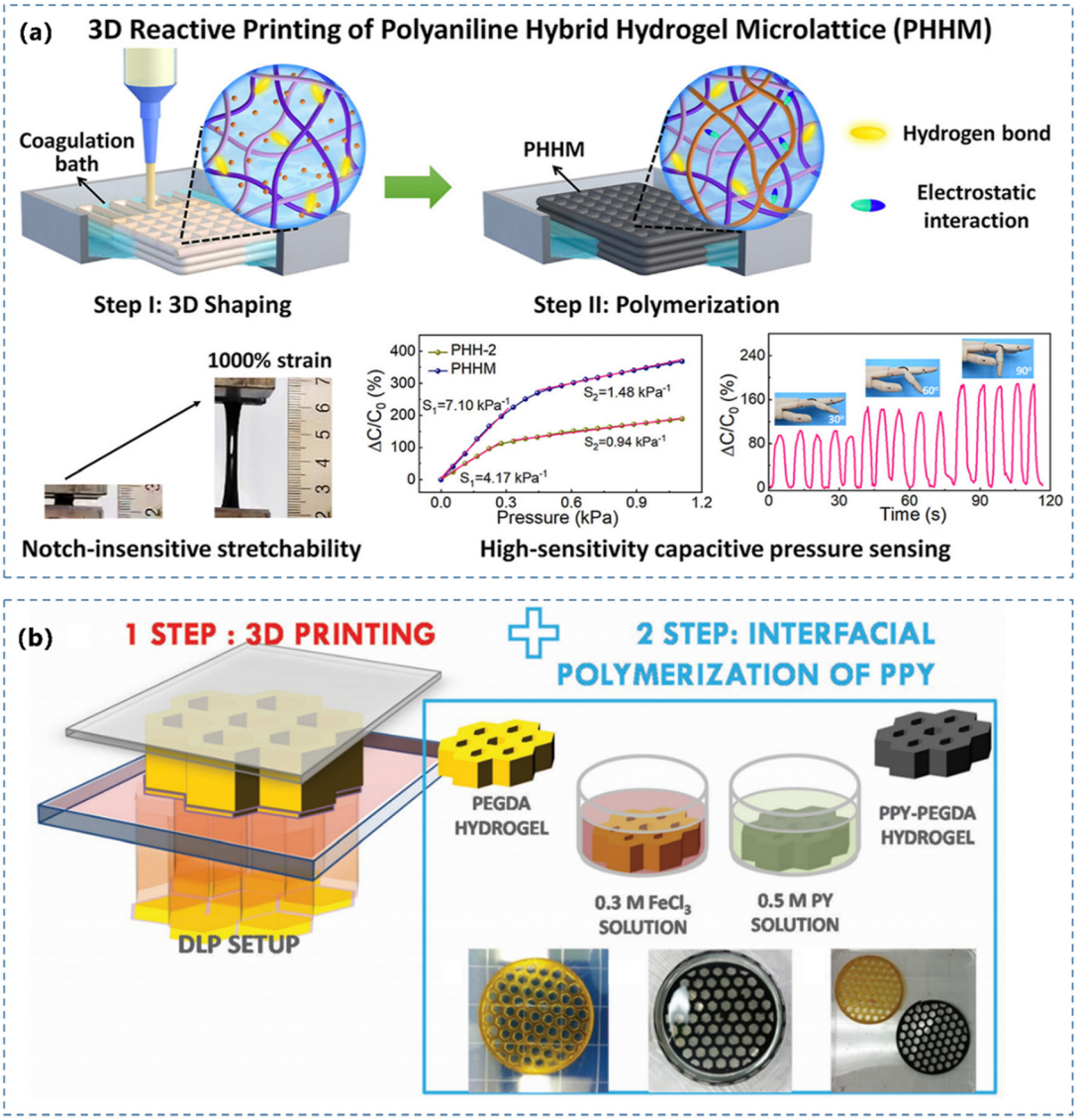

Fig. 4 (a) Schematic of the preparation of 3D reactive printing of the intrinsically stretchable PANI hybrid hydrogel with pressure sensing performance. Reprinted from ref. 120 with permission. Copyright 2022 Elsevier. (b) Sketch of a light-based 3D printing based preparation process for the conductive hydrogel hybrids. Reprinted from ref. 121 with permission. Copyright 2018 John Wiley and Sons.

of the CPs or CP precursors. The applied pressure forces the hydrogel to flow, hence introducing shear forces, which allow material deposition in the desired patterns.[118] A procedure consisting of rapid cryogenization, lyophilization and redispersion has been developed by Yuk,[119] to achieve the printable PEDOT:PSS hydrogels with suitable rheological properties, thus to secure high resolution and high aspect ratio microstructures.

The 3D printing route can achieve electroactive CPHs with complex and defined geometry, by *in situ* polymerizing CPs confined in a matrix framework. Yue *et al.*[120] mixed PAA, poly(ethylene oxide) (PEO) and aniline monomers to prepare a high-viscosity solution (Fig. 4a) as an ink for 3D printing. The resulted CPH presented a large stretchability, high fatigue resistance and a high sensitivity (7.10 kPa^{-1}). Besides extruding the hydrogel precursors, light-based 3D printing has also been widely used to fabricate CPHs. Jordan *et al.*[117] demonstrated a stereolithography 3D printing strategy for constructing architected CPHs with complex lattice structures by manipulating the properties of precursor solution. The light-based 3D printed hydrogel precursor can also serve as the structural template for absorbing the CP monomer. Fantino *et al.*[121] coupled light-based 3D printing with interfacial polymerization to obtain electroactive hydrogels with complex and defined geometry (Fig. 4b), using a digital light processing 3D printing system to fabricate a poly(ethylene glycol)-diacrylate (PEGDA) 3D structure first, by subsequently polymerizing the pyrrole monomer to create a conductive phase.

3. Network structure of CPHs

So far, many strategies have been established to deliver CPHs for WSs, which provide a broad perspective on designing and

fabricating specific CPH structures. We classify these network structures into three categories: (i) direct crosslinking of the CPs and then constructing single component CPHs;[122] (ii) doping or blending of the CPs into the insulting polymer matrix, forming a conductive network with nanostructures embedded relatively uniformly. This structure is called a CP nanocomposite hydrogel, which generally possesses better interactions between the hydrophilic polymer matrix and CPs, thus enhancing the mechanical properties;[123,124] (iii) double-network CPHs by composing the interconnected CPs and insulting polymer networks. The first network usually is a hydrophilic flexible matrix and hosts the polymerization of a conductive second network,[86,125] which is a crosslinked, modestly stretched network acting as an electronic transfer pathway.[126]

3.1. Single component CPHs

The delocalized π-electron system along the polymer backbone of the CP leads to the inherent rigid macromolecular chains. The traditional method to construct single component CPHs is to introduce small molecules with multi-functional protonic acid groups.[127] Recently, molecules with multiple functional groups have been reported to crosslink CP chains, resulting in a 3D network structured CP composite hydrogel. Superior to other dopants, phytic acid molecules can link to multiple PANI chains, generating a strongly crosslinked structure (Fig. 5a).[92,128] As described in Section 2.1.2, phytic acid (PA) is adopted as the gelator and the dopant in the synthetic process of PANI, which possesses a unique structure of several anionic phosphate groups, to initiate a mesh-like hydrogel network. Bao and co-workers[55] used phytic acid as PANI's cross-linker

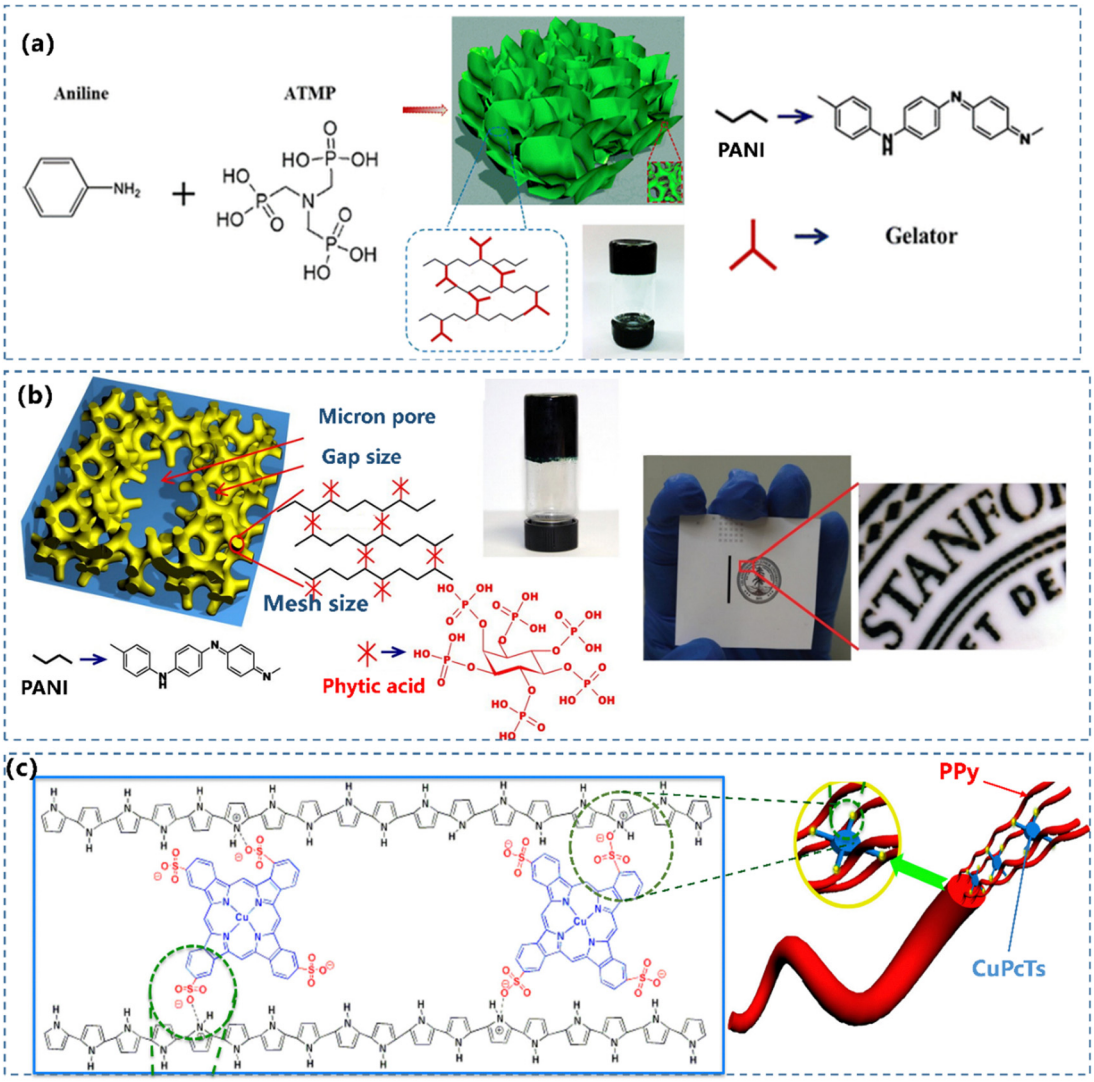

Fig. 5 (a) Schematic illustration of the formation of a 3D nanostructured PANI hydrogel and a photograph of the PANI hydrogel in a glass vial. Reprinted from ref. 92 with permission. Copyright 2016 Springer Nature. (b) Chemical structure and morphological characterization of a phytic acid gelated and doped polyaniline hydrogel. The photograph of an ink-jet-printed image on a piece of glossy photo paper. Reprinted from ref. 55 with permission. Copyright 2012 National Academy of Sciences. (c) Illustration depicting the controlled synthesis of CuPcTs doped PPy hydrogel. Reprinted from ref. 91 with permission. Copyright 2015 American Chemical Society.

and dopant, to generate a PANI hydrogel possessing a direct conductivity of 11 S m^{-1} (Fig. 5b). Similar to PA, disc-shaped liquid crystal copper phthalocyanine-3,4′,4″,4‴-tetrasulfonic acid tetrasodium salt (CuPcTs)[91] with tetra-functional groups was used to prepare a morphology-controlled nanostructured PPy hydrogel (Fig. 5c).

Besides the cross-linking of inherent rigid polymeric chains of CPs, elastic and conductive PPy hydrogels with a mono-phase were synthesized by Zhang's group using a unique secondary growth mechanism.[129] The formation of PPy occurred immediately upon the addition of an oxidant to realize the incipient network *via* π–π interactions with low joint density. The insoluble PPy chains aggregate into spherical particles, coupling with the unreacted pyrrole monomer formed protruded branches, resulting in a 3D building block. The optimized PPy hydrogel can be compressed by over 70%, and a fast full recovery within 30 seconds. This extremely elastic PPy hydrogel opens a window for developing elastic conducting hydrogels with applications in environmental engineering, biosensors, and regenerative medicine.

3.2. CP nanocomposite hydrogels

Combining CPs with amphipathic molecules to increase the dispersibility of CPs is an efficient option to obtain high performance CPHs.[130,131] The CPH can be equipped with multiple characteristics, allowing both materials to retain their respective properties.[132] There are two combinations of CPs and amphiphilic molecules: (1) to induce the functional polymer with hydrophobic groups into the hydrogel, and associate the hydrophobic groups and CPs, thus dispersing the CPs uniformly in hydrogels, resulting in a continuous conductive network for CPHs (Fig. 6a).[85,133] (2) To complex the CPs with hydrophilic molecules by non-covalent bonds to produce water-soluble CPs.[134]

For the first strategy, the hydrophobic interaction in hydrogels prevents the CP nanoparticles from aggregating. The modification of CPs with amphiphilic molecules to generate micro or nano-scale micelles can effectively support the dispersion of CPs into a homogeneous conductive component, to initialize the uniformly crosslinking to achieve a continuous conductive network.[137] Sun *et al.*[135] designed a CPH-based strain sensor by introducing PANI coated silica core–shell particles (SiO_2@PANI) into an acrylamide–lauryl methacrylate copolymer (P(AM/LMA)) matrix (Fig. 6b), where the hydrophobic interaction between the hydrophobic LMA in the P(AM/LMA) chains and the SiO_2@PANI core–shell particles induced a stable and continuous conductive network. This resulted in favourable electrical conductivity, high strain sensitivity with a gauge factor (GF) of 10.407 at 100–1100% strain, a fast responsiveness (300 ms), and excellent durability (300 cycles).

Another approach is to produce soluble CPs by complexing them with hydrophilic molecules. The popularly used CP nanocomposite hydrogel is the PEDOT:PSS hydrogel,[136,138,139] with PEDOT domains placed in an electrically insulating PSS matrix under a loosely crosslinking association by hydrogen bonding. Zhao *et al.*[39] reported a CP based hydrogel technique by interconnecting networks of PEDOT:PSS nanofibrils with excellent electrical, mechanical, and swelling properties (Fig. 6c). The obtained pure PEDOT:PSS hydrogel fulfilled the desired properties for bioelectronic applications, including high electrical conductivity, low Young's modulus, and tunable isotropic/anisotropic (de-)swelling in wet physiological environments. Apart from the hydrophilic polymers, hydrophilic micro- or nanomolecules are also imported to enhance the solubility of CPs. Lu's group[85] doped catechol/quinone contained sulfonated lignin to CPs to prepare a series of water-soluble CPs, including PANI, PPy and PEDOT. The resulted hydrogel exhibited high conductivity with uniformly distributed hydrophilic CPs and a well-connected electric pathway. However, the CP nanocomposite hydrogel is vulnerable to the phase separation between the CPs and the hydrophobic polymer matrix, due to the intrinsic incompatibility.

3.3. Double-network CPHs

In the double-network CPHs, the system interlinks two polymer networks with adverse or immiscible properties to enable unique features such as high mechanical robustness, extreme stretchability, and bespoken chemical functionality.[140–142] The double-network CPHs usually contain a densely cross-linked, fully stretched network that acts as a rigid skeleton, while the other network is cross-linked sparsely.[143,144] The interlinks between two networks can be facilitated by covalent cross-linking and/or non-covalent bonding (*i.e.* hydrogen bonding and hydrophobic or ionic interactions).[145,146] The dynamic cross-linking network enables the CPHs to form a reconfigurable structure with large deformation, which is critical for the mechanical properties, conductivity and sensing performance.

The modulations of the topology for hydrophilic polymers and physically/non-covalent contacts between the networks can regulate the properties of CPH-based WSs.[54,148] Chen's group used 2-ureido-4[1*H*]-pyrimidinone (UPy) to cross-link PANI in a hydrogen-bonded PSS network (Fig. 7a).[78] Shi *et al.*[147] synthesized PNIPAM/PANI and PNIPAM/PPy CPHs using the same process. Both the obtained CPHs were equipped with an interpenetrating binary network structure and possessed a continuous transporting path for electrons. The PNIPAM/PANI and PNIPAM/PPy CPHs exhibited different electrical conductivities and thermoresponsive sensitivities, owing to the different properties between PANI and PPy (Fig. 7b). Typical hydrophilic polymers including soft polymers (*i.e.* PVA,[51,76,77] PNIPAM[147,149] and PAm[150,151]) and rigid polymers such as crosslinked cellulose nanocrystals (CNCs)[56,152,153] can be utilized to construct double-network CPHs. Ma *et al.*[154] fabricated double-network CPHs by inducing supramolecular interactions between boronic acid groups on PANI and hydroxy groups on PVA. Because of the efficient energy dissipation, the CPH achieved good mechanical properties with a Young's modulus of 27.9 MPa, a tensile strength of 5.3 MPa, and an elongation at break of 250%. Tang' group[86] developed a synergistic dual network hydrogel PANI-P(AAm-*co*-AA)@Fe^{3+} composed of an iron-coordinated poly(AAm-*co*-AA) network and a conductive PANI network with adjustable mechanical properties and high sensitivity (Fig. 7c). The host–guest interaction between β-cyclodextrin (β-CD) and PANI improves PANI's compatibility in a hydrogel substance,

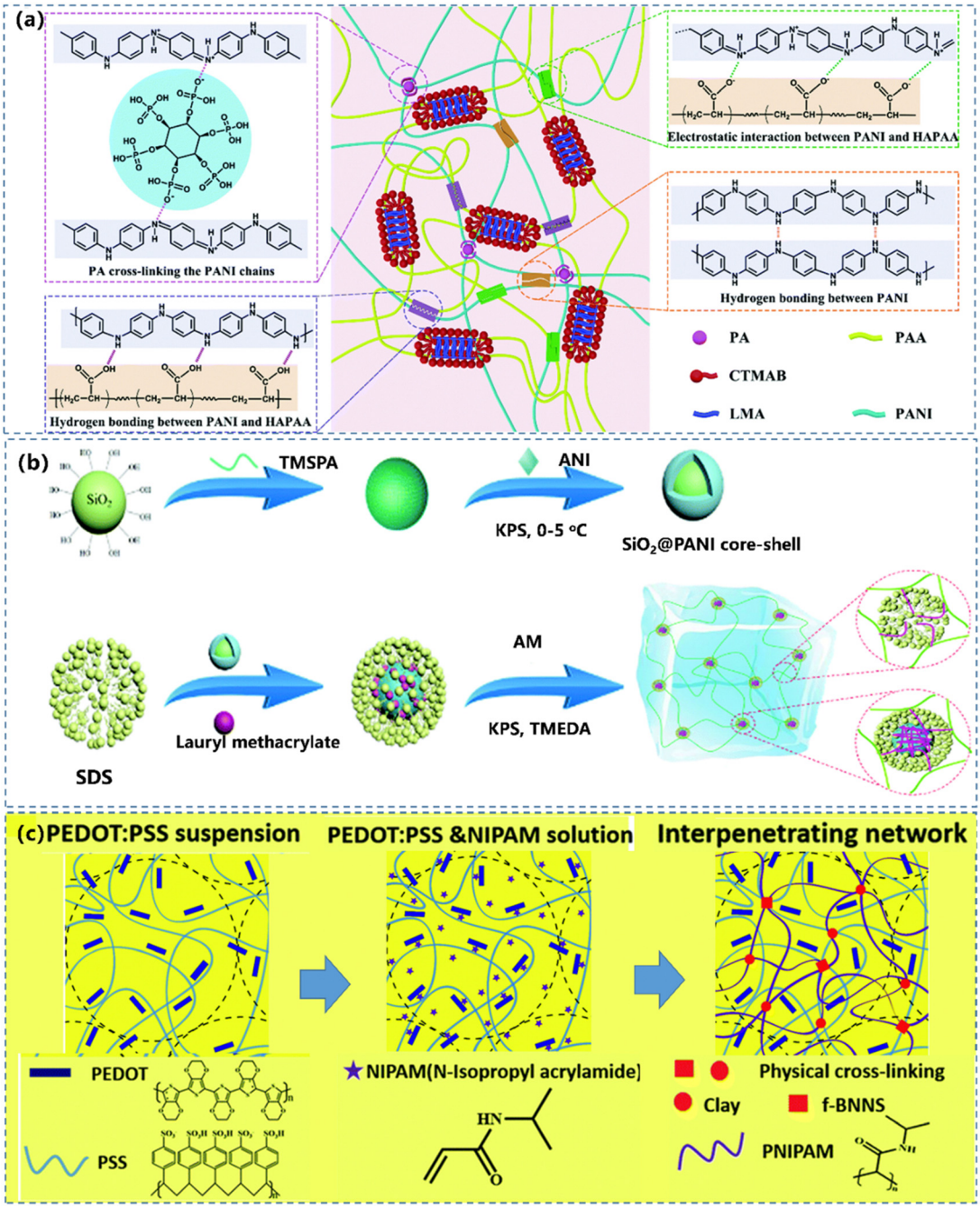

Fig. 6 (a) Hydrophobic association of the physically cross-linked PAAN hydrogels and the interactions within the gel. Reprinted from ref. 133 with permission. Copyright 2021 Royal Society of Chemistry. (b) The preparation of a SiO_2@PANI-P(AM/LMA) hydrogel. Reprinted from ref. 135 with permission. Copyright 2021 Royal Society of Chemistry. (c) Fabrication process of f-BNNS/PEDOT:PSS/PNIPAM hydrogels. Reprinted from ref. 136 with permission. Copyright 2019 Royal Society of Chemistry.

and leads to the formation of homogeneous interpenetrating networks.

4. Properties and applications of CPHs in wearable electronics

Significant progress has been made in endowing CPHs with the desired characteristics in the application of WSs,[87,155–157] such as conductivity, mechanical properties, self-healing ability, self-adhesiveness, and biocompatibility.[158,159] Recent advancements in this area are summarized in this section.

4.1. Properties of CPHs

4.1.1. Mechanical properties. The stress localization in soft electronics frequently happens during operation to cause the malfunction and system failure for the device, due to

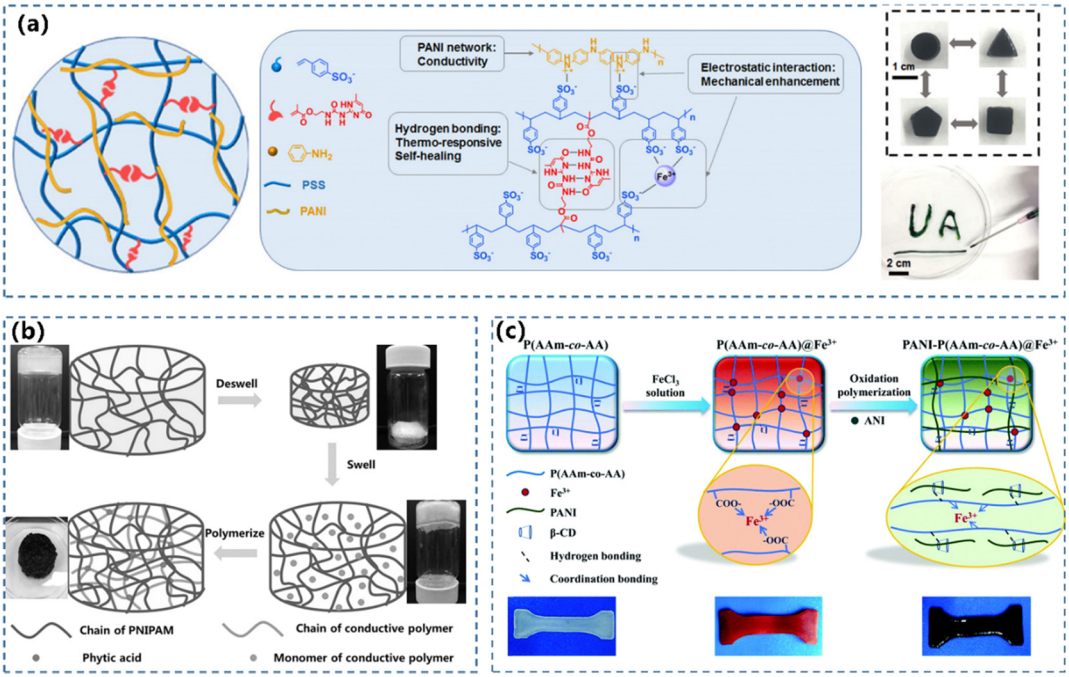

Fig. 7 (a) The formation mechanism of supramolecular conductive PANI/PSS-UPy hydrogels and optical images of the hybrid hydrogels molded into different shapes and injected through a needle. Reprinted from ref. 78 with permission. Copyright 2019 American Chemical Society. (b) Synthesis of a hybrid hydrogel composed of PNIPAM and conductive polymers. Reprinted from ref. 147 with permission. Copyright (2015) John Wiley and Sons. (c) Illustration of the fabrication of a PANI-P(AAm-*co*-AA)@Fe^{3+} hydrogel. Reprinted from ref. 86 with permission. Copyright 2022 Royal Society of Chemistry.

stretching, bending, tapping, or pressing.[159–162] Therefore, mechanical qualities are usually crucial to determine the performance of CPH-based WSs, where numerous attempts have been made.[69,72,151] Considering the rigid nature of conductive polymers, the constructive hydrogels are susceptible to long-term deformation, leading to fatigue and fracture after cyclic deformation.[163] The formation of an interpenetrating polymer hydrogel is believed to be a good strategy to endow the CPHs with long-term durability in the mechanical properties, whereas the soft chain network can withhold the high elasticity of the interpenetrating network structure.[164] Sun and co-workers[165] proposed a dually synergetic network hydrogel composed of the soft polymer PAAm and the rigid conductive polymer PEDOT:PSS, the soft chains mechanically interlock with the rigid chains to provide the CPHs with a ultra-wide sensing range of 0–2850%.

Upon deformation, the dynamic noncovalent bonds (such as hydrogen bonds and the gelation network) normally behave as fragile, to serve as reversible "sacrificial bonds" to participate in energy dissipation *via* dissociation and/or reconstruction. Outstanding mechanical properties could be achieved *via* the mediation of inter- and intramolecular interactions based on the chemical and physical bonds. Dynamic interactions are prone to break to dissipate energy when CPHs are stretched, ensuring the hydrogels a fully and speedy recovery to their original states.[166] Xu *et al.*[167] fabricated a polysaccharide-based conductive hydrogel through the fine-tuning at molecule-scale between conductive PEDOT and other polymers, which contributes to the significant improvement of mechanical behaviours.

4.1.2. Self-healing. Self-healing is an appealing feature of CPHs to allow the quick restoration of mechanical and electrical characteristics, an extended lifespan of CPH sensors and a dramatical reduction on the cost (Fig. 8a and b).[136,169–172] The self-healing mechanisms can be classified into two types, intrinsic and extrinsic. The addition and polymerization of healing agents, such as some natural polymers like gelatin, carrageenan, and agar, is the fundamental extrinsic self-healing mechanism.[173,174] The intrinsic self-healing hydrogels are usually double-network hydrogels that can undergo reversible fracture and reconstruction. The main driving forces are the dynamic non-covalent bonds (*i.e.*, hydrogen bonds, electrostatic bonds, hydrophobic interactions, π–π interactions, and host–guest interactions) and supramolecular interactions.

Incorporating CPs into the supramolecular network is effective to bring self-healing features to the hydrogel, because multiple dynamic interactions can be established between the conductive polymer and the other polymer network. Based on the good hydrogen donor of PANI, the self-healing PANI-based hydrogel was fabricated by introducing the hydrogen acceptor PAAm.[175] The fractured PANI hydrogel can be restored to its original structure ascribed to the reconnection of hydrogen bonds. Li *et al.*[168] prepared double network CPHs through integrating rigid PANI chains with flexible sodium methallyl sulfonate functionalized poly (thioctic acid) polymer chains (Fig. 8c). In addition, reversible covalent interactions are also

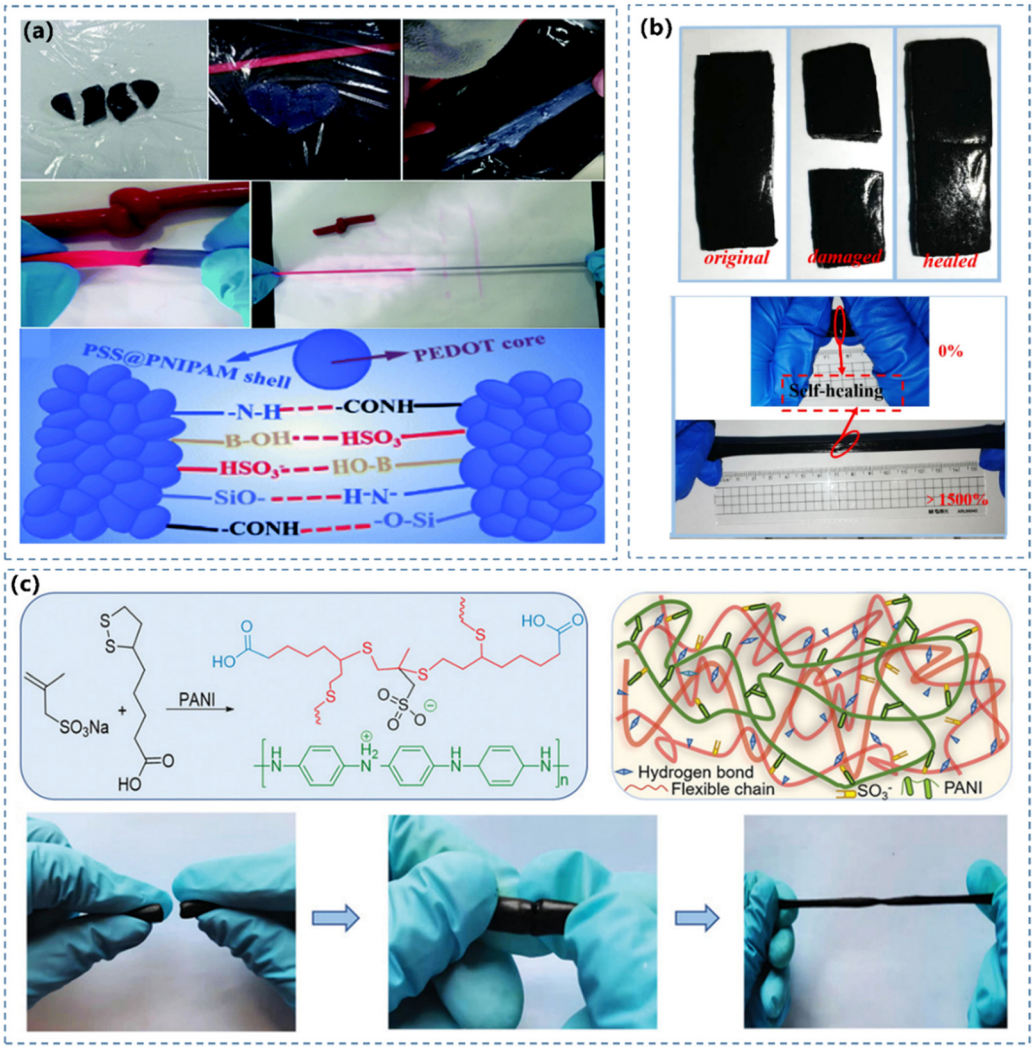

Fig. 8 (a) Self-healing of the obtained hydrogel and the illustration of the mechanism.[136] Reprinted from ref. 136 with permission. Copyright 2019 Royal Society of Chemistry. (b) Self-healing test of CNC-PANI/PVA hydrogels with a healing time of 30 s. Reprinted from ref. 153 with permission. Copyright 2020 Elsevier. (c) Diagrammatic illustration of the structure and characterization of the CPHs. Reprinted from ref. 168 with permission. Copyright 2021 John Wiley and Sons.

intriguing for imparting the hydrogel with self-healing capability. Wang *et.al.*[176] prepared self-healing CPHs with long lifespan by rearranging the Diels–Alder covalent bonds between polymer chains.

Integrating self-healing capability and mechanical toughness together in a single structure is intriguing due to the conflicting demands. Strong molecular interactions are indispensable for imparting hydrogels with robust toughness, whereas the high cross-linking density of networks is detrimental to the mobility of polymer chains, restricting the possibility of the self-healing of hydrogels. As such, most self-healing CPHs are fabricated based on the incorporation of multiple weak molecular interactions, which will sacrifice the mechanical strength and toughness of CPHs. In light of this trade-off effect, self-healing CPHs that balance self-healing and the mechanical properties (toughness and stretchability) were delivered by Su *et al.*[133] They constructed dynamic interfacial interactions (including hydrogen bonding and electrostatic interactions) between the conductive PANI and hydrophobic association poly(acrylic acid) (HAPAA) network to elaborate interfacial interactions without sacrificing their self-healing capability. On one hand, the dynamic interfacial interactions constructed multiple energy dissipation mechanisms for endowing the CPHs with exceptional mechanical properties. On the other hand, the multiple reversible dynamic interactions between two networks can reassociate quickly after the break, therefore endowing the HAPAA hydrogel with good self-healing ability.

4.1.3. Self-adhesive. WSs with self-adhesive properties ensure a reliable and conformal contact with human skin, reduce the interface resistance and stabilize the stimuli detection.[177–181] To equip the CPHs with self-adhesiveness, the introduction of some moieties that can adhere to different substrates is of particular importance. The incorporating catechol-based

molecules for providing the hydrogel with adhesiveness that inspired by muscle has gained great attention.[163,182,183] Lu *et al.*[89] integrated catechol molecules to dopamine, to synthesize PPy-based CPHs. Catechol moieties imparted the hydrogel with excellent adhesiveness, and high conductivity due to the effective paving of conductive pathways based on the dopamine-decorated PPy nanofibrils. Meanwhile, through tuning the covalent and noncovalent contents, the dynamic network based on PEDOT:PSS can be well controlled. As such, the resultant CPHs exhibit durable adhesion with high electroconductivity and cytocompatibility.[167]

The hydrated environments (*e.g.*, sweating, raining and swimming) endanger the performance of WSs by deteriorating the interfacial adhesion.[184] Incorporating hydrophobic moieties into the hydrophilic polymer network is an effective way to tackle this challenge.[185] Gao and co-workers[186] designed a hydrogel with robust underwater adhesion and reliable fatigue-resistance capability, by copolymerizing hydrophilic monomers and hydrophobic monomers. The formation of hydrophobic aggregation expels the water and guarantees the direct contact of adhesion groups attached to the hydrogel with substrates. In addition, there is another approach to introduce several nanometer-thick hydrophilic adhesive layers onto the CHPs *via* the interpenetrating polymer network, to provide hydrogels with strong underwater adhesion without sacrificing their mechanical and electrical characteristics.[187]

4.1.4. Electrical conductivity. High electrical conductivity is always required for electronic readout purposes. CPHs are made up of CPs with intrinsic conductivity and soft hydrophilic polymer networks. The insulating hydrophilic polymer networks serve as scaffolds, while the CPs provide the conductive pathway. The electrical conductivity significantly affects the electrical transmission and sensitivity of CPHs. Chen's group generated an interpenetrating PANI/PSS network, with good conductivity, stretchability, and self-healing ability by optimizing the concentration of PANI.[78] Fu's group[54] demonstrated that the electron transit in hydrogels is dependent on the tunnelling effect when the induced CPs are at low concentrations. Continuous conductive networks can be established by further improving the concentration of PANI to reach their percolation threshold, and the PANI chains are contact with each other, thus creating electron transit channels with low resistance, leading to a high conductivity of 8.24 S m^{-1}.

The electronic conductivity originates from the unique conjugated π-structure of CPs, which are organic conductors that depend on electronic conductivity. There are two main methods to improve the conductivity of CPHs: on one hand, enhancing the content of CPs in CPHs could efficiently improve their conductivity, owing to that the isolated electronic transfer pathway gradually evolved into the 3D conductive network, which proved higher charge transport speed, leading to higher conductivity. For example, both Wang[80] and Jin[151] demonstrated that improved conductivity of CPHs can be obtained by enhancing the feeding ratio of the CP monomer, and the conductivities of the optimized samples are tens of times than that of the virgin hydrophilic hydrogels. The whole conductive networks are further created when the concentration of CPs is improved to their percolation threshold, forming relatively low-resistance paths for electron transportation due to the contact of conductive materials.[188] Notably, the conductivity of CPHs will approach to a plateau value once the content of CPs exceeds the percolation threshold. On the other hand, doping is a common process to improve the CPHs' electrical properties.[88] Doping CPs with proton acid creates bipoles and dipoles along the polymer chain, transferring more carriers in the form of electrons or holes, which significantly improves the conductivity of conducting polymers. Milakin *et al.* demonstrated that the higher content of the dopant leads to increased conductivity,[128] and this can be attributed to higher resistance to deprotonation of phytic acid doped PANI which occurs during washing of the resulting cryogels with water. Moreover, the conductivity of CPHs is highly dependent on the type and concentration of dopants. Wang *et al.*[91] synthesized PPy hydrogels with three different types of dopants and measured the conductivity of the obtained PPy hydrogels as 7.8, 0.4, and 0.06 S cm^{-1}, respectively.

4.1.5. Biocompatibility. The WSs can comprise various types of physical sensors, in detecting a change in a physical stimulus and then generating a signal to be measured or recorded. To accurately acquire human movement, it is essential to adhere the CHPs directly to human skin. Considering the direct contact between CHPs and the skin, endowing the CHPs with good biocompatibility is of critical importance.[189] CHPs have been developed as wound dressing,[89,190] tissue engineering[191] and WSs[153,192] due to their good biocompatibility and easy synthesis.

4.2. CPHs for wearable sensors

In general, the ideal conductive hydrogel for sensors should be stretchable, tough, conductive, self-healable, and highly sensitive to external deformations. CP chains are able to construct an ideal 3D interconnected conducting network for providing an all-organic, continuous conducting path compared to that of the noncontinuous, point-to-point connected conducting network derived from inorganic nanoparticles,[75] could be helpful for fabricating a press/strain sensor with high sensitivity and linearity, which are pivotal for the feasibility and accuracy of hydrogel sensors.[54] As compared with other conductive filler-based hydrogels, they usually show a nonlinear dependence of sensitivity on strain, presumably due to the damage of the noncontinuous conductive network during stretching.[193] Moreover, the organic and polymeric nature of CPs enables diverse chemical modification and cross-linking strategies, resulting in extraordinary flexibility and self-healing ability.[22,133,194] In contrast, high stiff fillers such as metallic/carbon materials would decrease the self-healing ability of the hydrogel by restricting the mobility of polymer chains, the ability to restore equivalent sensing functions after healing from severe damage is also limited. Island-type distributed inorganic fillers in the hydrophilic polymer matrix are also challenging to balance the trade-offs among mechanical, electronic, and self-healing properties. A detailed list of examples of CPH-based sensors can be found in Table 2.

Table 2 A detailed list of examples of CPH-based sensors

Application	CPHs	Conductivity	Dopants	Stretchability	Specific device metrics	Ref.
Press/strain sensor	PAM/gelatin/PEDOT:PSS	—	PSS	2850%	GF = 0.46–1.58	165
	poly(HEAA-*co*-SBAA)/PEDOT:PSS	0.625 S m^{-1}	PSS	4000–5000%	GF = 2	195
	PANI/PVA/PA/GA	3.4 S m^{-1}	PA	670%	GF = 3.4	77
	PPy/PU	0.055 S m^{-1}	—	592%	—	204
	PEDOT:PSS-PVA	—	PSS	~370%	GF = 4.07	32
	PANI/PAA/glycerol	—	PAA	~1500%	TCR = −0.0164 $°C^{-1}$	22
	PNIPAM/CMCS/MWCNT/PANI	5.5 S m^{-1}	HCl	~400%	—	205
	HAPAA/PANI/Gly	~3 S m^{-1}	PAA	2378%	TCR = −1.28% $°C^{-1}$	206
	PNIPAM/PPy	0.8 S m^{-1}	PA	—	—	147
Humidity sensor	PEDOT:PSS	—	PSS	—	RH range: 2–90%	207
	CCNF/PEDOT:PSS	58 mS m^{-1}	PSS	929%	RH range: 0–85%	208
Gas sensor	CeO_2@PANI	—	PA	—	6.5–50 ppm (NH_3)	209
	PEDOT:PSS/IrO_x	—	PSS	—	17–7899 ppm (NH_3)	210
	PEDOT:PSS	—	PSS	—	13–21 vol% (O_2)	211
Energy storage system	PANI	0.11 S cm^{-1}	PANI	—	450 F g^{-1} (0.5 A g^{-1})	55
	PANI/PA/PVA	91.0 mS cm^{-1}	PA	180%	2097 mF cm^{-2} (2 mA cm^{-1})	99
	PPy-CPHs	2.3 S cm^{-1}	p-TSA	—	560 F g^{-1} (0.75 A g^{-1})	212
	PEDOT-PVA	0.9 S cm^{-1}	Boric acid	>400%	75.9 F g^{-1} (0.29 A g^{-1})	213
	PEDOT:PSS/silk fibroin	1 mS cm^{-1}	PSS	—	1.1 F cm^{-2} at 0.5 mA cm^{-1}	214

A range of CPH based WSs have been developed that can respond to pressure, temperature, and metabolites, among other stimuli.[188,195–198] Various advanced wearable sensors possess the ability to detect at least two stimuli at the same time. In this section, we review recently developed sensing modes in CPH based WSs, such as resistive, capacitive, and triboelectric type sensing modes. Moreover, the recent advances in wearable sensor applications including thermal, press/strain sensors, temperature and pressure/strain dual-functional sensors, gas sensors and humidity sensors will be reviewed.

4.2.1. Sensing mechanism. CPH-based WSs can adaptively respond to the human motion.[199] The interconnected conductive network and/or interactions between the CP chains and the hydrophilic polymer matrix in CPHs enhance the WSs' responsiveness. Two representative categories are resistive sensors and capacitive sensors.

Resistive sensors. The resistive sensing mode is one of the most widely used sensing modes in WSs owing to its relatively high sensitivity[200–202] (Fig. 9a). This type of WSs, usually made by hydrogels with low concentrations of CPs,[203] depends on the change of configuration in conductive networks, and brings high sensitivity *via* the contact-resistance effect and the tunnelling effect. Resistive sensors can be divided into two categories: (1) piezoresistance sensors, typical for sensing press/strain and (2) thermoresistive sensors for sensing temperature.

The mechanical deformation on piezoresistance sensors leads to the change in resistance.[125,215] Under a small deformation, the tunnelling distance of the conductive network in the piezoresistance sensor exhibits a minute variation. Subsequently, some tunnelling channels increase linearly in tunnelling distance with an increase in the applied force. A stronger signal is produced when the tunnelling distance exceeds the cut-off distance. Some direct connections between the conducting materials are broken.[216,217] The thermoresistive typed sensor can rapidly respond to the thermal stimuli by changing its own resistance. The sensing mechanism of thermosensitive CPHs can be classified into two groups: (1) CPH-based WSs to detect the body temperature with a reversible temperature response.[218–220] The mechanism is fulfilled by combining the CP with a thermal-sensitive polymer such as PNIPAM,[149] to switch the conductive network's tunnelling distance by harnessing the thermal-sensitive polymers' capacity. (2) CPs

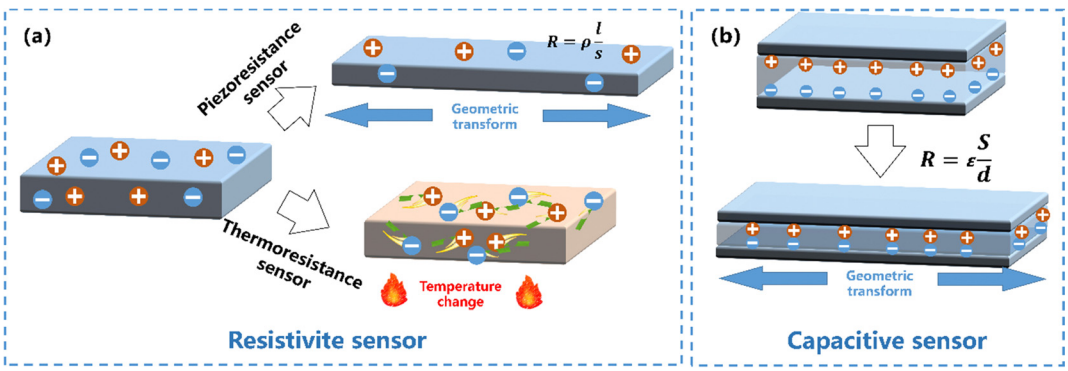

Fig. 9 Schematic illustration of the structure and working mechanism of a (a) resistive sensor, and (b) a capacitive sensor.

inherently have excellent thermal expansion,[22,221] to rapidly react to the instantaneous temperature fluctuation of the human body. The temperature increase quickly accelerates carrier hopping between inter-fiber junctions, resulting in an ultrafast response in the signal.[222]

Capacitive sensors. Compared to a resistive sensor, a capacitive sensor possesses higher linearity, enhanced hysteresis, and faster response, for sensing press/strain.[223] A capacitive sensor can be constructed by sandwiching a dielectric layer between two conformable conductive layers[113,120] (Fig. 9b). The formula $C = \varepsilon S/d$ can be used to determine the capacitance (C) of a capacitive sensor, where ε, S, and d correspond to the permittivity, contact area, and thickness of the dielectric layer, respectively. The sensors will respond to the external stimuli by adjusting the interval between two parallel plates, resulting in an output capacitance signal change.[224] For example, Mo and coworkers[225] demonstrated a capacitive-type strain sensor based on an alginate/PAAm hydrogel and conductors and a semi-interpenetrating network structural organogel dielectric. The obtained capacitive strain sensor possessed extremely operational stability and the fast response speed for detecting small physiological signals and large-range human motions real-timely. However, for hydrogel-based press/strain sensors, most of them in the literature belong to resistance sensors while a minority are capacitive sensors.[30] Notably, there are few CPH based capacitive press/strain sensors as of today; we think that this is mostly due to that the sensing mechanism of the capacitive sensor is oriented from the electronic double layer (EDL) formed at the electrolyte–electrode interface,[226] while the Faraday pseudocapacitive behavior of the CPs will disrupt the linear sensing signal of the EDL capacitive sensor.

4.2.2. Sensing applications

Pressure/strain sensors. Pressure/strain sensors are popular and generate an electrical signal dependent on either pressure or strain (Fig. 10a). The CPH-based press/strain sensors are normally made by interpenetrating conductive polymer-based hydrogel networks by cross-linking various non-covalent bonds.[112,227–229] Sensing sensitivity, response speed, and long-term durability under force loading are key merits of pressure/strain sensors, where a rapid response and low hysteresis are particularly needed.[125,230]

The piezoresistive sensors are 'star' players in pressure/strain CPH sensors, due to the facile fabrication, simple read-out mechanism and superior sensitivity.[54,231] The piezoresistive effect is a mainstream mechanism in the pressure/strain sensor, and a higher value of GF can endow a better precision of the sensation (Fig. 10b). Zhang's team[195] synthesized a conductive hydrogel by interpenetrating conductive PEDOT:PSS polymers and zwitterionic poly(HEAA-*co*-SBAA) polymers (Fig. 10c), capable of changing its conductivity under deformation. Xu's group[232] prepared a PANI based hydrogel with potential for large-area and low-cost fabrication of WSs. The prepared sensor exhibited a sensitivity of 37.6 kPa^{-1} in the range of 0–0.8 kPa and presented ultrahigh sensitivity even under a high load (1.9 kPa^{-1} at 5 kPa). Bao's group[233] developed an ultra-sensitive pressure sensor based on an elastic, microstructural conducting polymer thin film made from a PPy hydrogel. The micro-patterned PPy-based hydrogel pressure sensor has an ultrahigh sensitivity in the low-pressure regime and can detect pressures as low as 1 Pa.

Recently, triboelectric nanogenerators (TENGs) lead an energetic trending development of WSs by not only efficiently harvesting the everyday body motion and powering various portable electronics, but also detecting the pressure/strain stimulus in the process of generating electricity. The hydrogel-based TENG sensors generate potential signals without any external power supply with a number of advantages, such as light weight, prominent mechanical stability and facile cost-effective device structure. Shen and co-workers[165] used PEDOT:PSS as the conducting component, combined the rigid physically cross-linked gelatin, tough chemically cross-linked PAAm to construct stretchable and conductive hydrogels (Fig. 10d). The device not only served as a stretchable TENG for effective energy harvesting and a self-powered wearable device, but also exhibited favorable pressure/strain sensing ability, including a high sensitivity (GF = 1.58), a rapid responsiveness (200 ms), a broad sensing range of 0–2850%, and a stable/reproducible output sensing signal (1200 cycles). It has also been shown that the contact area dependent electrical response to an applied pressure in TENGs can be utilised directly to measure the contact pressure.[234–236]

Temperature sensors. The temperature of the human body has been a primary parameter to indicate the status of the fitness of an individual.[237] The precise, continuous and real-time monitoring of temperature for the human body is critical to reveal the healthy state and to provide evidence for the early diagnosis of diseases such as cardiovascular diseases, pulmonological diagnostics and infectious diseases such as COVID-19.[238] Among these developed CPHs,[239–241] CPHs for detecting temperature through resistive changes have attracted considerable attention. The conventional fabrication of CPH temperature sensors is to combine a conductive polymer with a thermal sensitive polymer. The CPHs' bulk electrical resistivity responds to absolute temperature, with the slope of curve relating to sensitivity or the temperature coefficient of resistance. Yu *et al.*[147] synthesized thermally responsive and conductive hydrogels by cross-linking PANI with phytic acid in a PNIPAM matrix. The resulted PANI/PNIPAM hybrid hydrogels demonstrated a unique combination of excellent electrical conductivity, high thermo-responsive sensitivity, and increased mechanical capabilities.

Temperature and pressure/strain dual-functional sensors. The transfer speed of carriers between inter-molecular junctions can quickly increase as the temperature increases. The conductivity and temperature coefficient of resistance were improved since the thermal vibration triggered electrons could produce a tunnelling current through nearby PANI junctions.[149,193] Ge *et al.*[22] reported a highly stretchable and self-healing hydrogel-based sensor with exceptional stretchability, area expansion, and healing efficiency (Fig. 11a). It had a gauge factor of 18.28, a

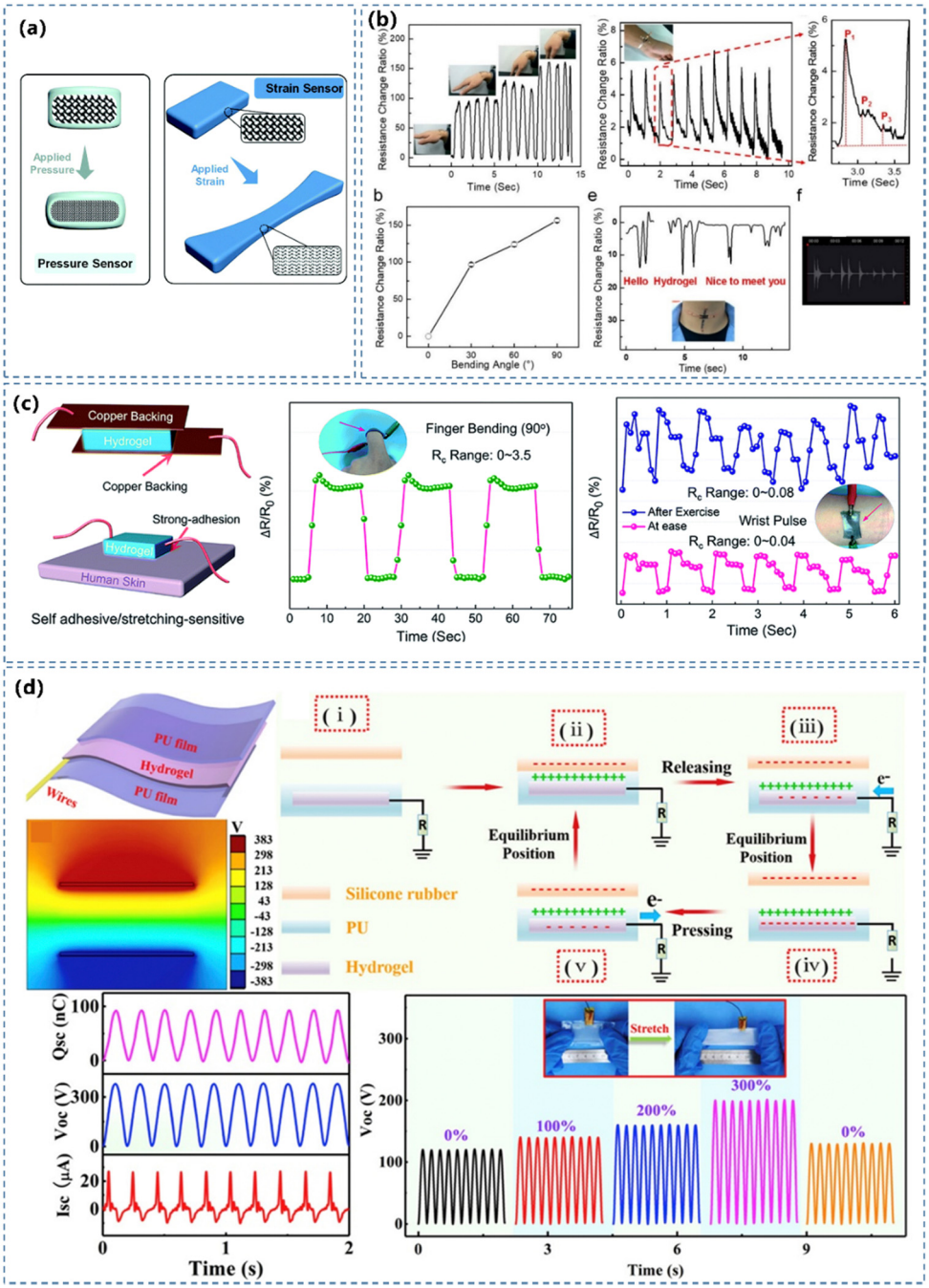

Fig. 10 (a) Schematic illustration of pressure and strain sensors. Reprinted from ref. 125 with permission. Copyright 2020 Royal Society of Chemistry. (b) Signals from CPH sensors on the wrist, the wrist pulse and on the throat of a volunteer speaking "Hello", "Hydrogel" and "Nice to meet you". Reprinted from ref. 54 with permission. Copyright 2018 American Chemical Society. (c) Schematic illustration of stretching-induced and pressure-induced hydrogel strain sensors and sensing performance. Reprinted from ref. 195 with permission. Copyright 2020 Royal Society of Chemistry. (d) CPH-based highly stretchable (300% strain) TENG device and its energy harvesting performance achieved a short circuit current (I_{SC}) of 26.9 μA, an open circuit voltage (V_{OC}) of 383.8 V and a short-circuit transferred charge (Q_{SC}) of 92 nC. Reprinted from ref. 165 with permission. Copyright 2020 Elsevier.

broad sensing range, a lower detection limit, an excellent thermal responsiveness ($-0.0164\ ^{\circ}C^{-1}$), a distance-dependent thermosensation ($-0.022\ ^{\circ}C\ mm^{-1}$) and a high temperature resolution of 2.7 °C. Hao's team[242] reported strain and temperature dual-functional CPH based WSs by combining the thermosensitive TEMPO-oxidized cellulose/PANI networks in the hydrophilic hydrogel polymer matrix through hydrogen bonds and electrostatic interactions (Fig. 11b). They coupled the charge transfer caused by the spatial position and the tunneling current activated by thermal vibration to detect human motion and temperature simultaneously. By leveraging the superposed signals discrimination ability of CPs, the obtained CPHs exhibited excellent

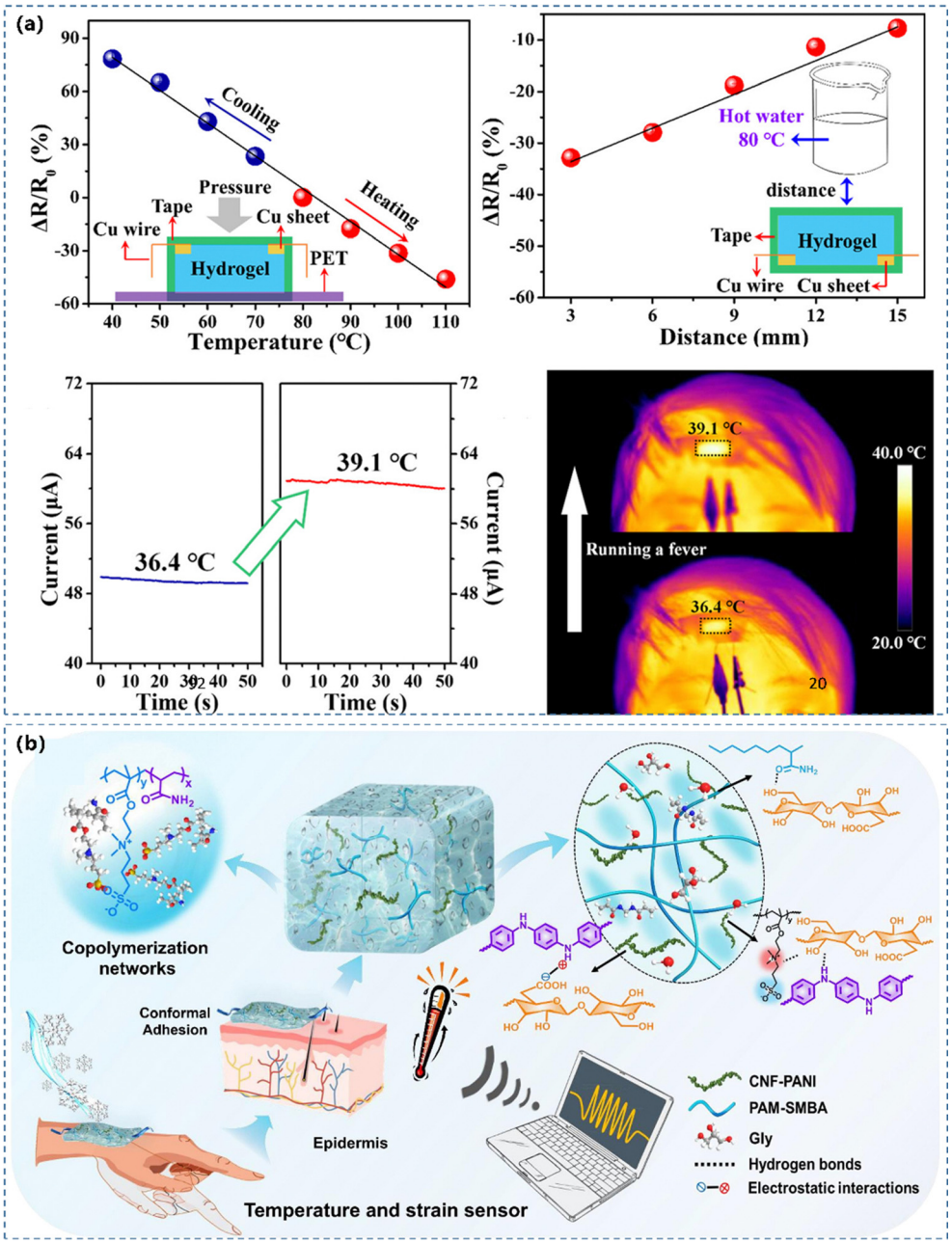

Fig. 11 (a) A temperature sensor serves to monitor a human forehead's temperature. Reprinted from ref. 22 with permission. Copyright 2020 American Chemical Society. (b) The design of a PANI based hydrogel with strain and temperature responsiveness. Reprinted from ref. 242 with permission. Copyright 2022 Elsevier.

outstanding thermosensation (TCR = 2.01% $°C^{-1}$) and strain sensitivity (GF = 1.25).

Gas sensor. As gases are considered as biomarkers of human diseases,[243–245] developing wearable gas sensors that can precisely detect specific gases at low concentrations has enormous value for human healthcare.[246–248] PANI undergoes significant changes in its electric characteristics upon doping/dedoping with amines, making it an excellent material for the construction of gas sensors.[249] For example, Wang *et al.*[209] reported a room-temperature CeO2@PANI hydrogel based NH_3 gas sensor, which showed a high response (6.5 to 50 ppm of NH_3) and a short detection time (a response of 6.5 and a response time 57.6 s). The improved sensing performances can be attributed to the p–n heterojunction within the core–shell structure. Notably, the obtained CPH sensor exhibited excellent long-term sensing stability, mainly due to the doping and crosslinking effects on the polymer chains. Furthermore, one of the greatest and least recognized risks to human is oxygen deprivation in confined places. Wearable oxygen sensors for detecting reduced oxygen levels are urgently needed for protecting people from injuries and death.[250,251] Decataldo and

co-workers[211] developed a wearable oxygen sensor at room temperature based on PEDOT:PSS. The fast O_2 solubilization in the hydrogel allowed for gaseous oxygen transduction in an electrical signal thanks to the electrocatalytic activity of PEDOT:PSS. The obtained CPH gas sensor exhibited a low power consumption of 30–40 μW.

Humidity sensor. Humidity is considered one of the most effective variables for respiration monitoring,[252] and high-performance humidity sensors have been paid increasing attention over the past years in the field of health assessment and disease prediction due to their advantages of fast response, high sensitivity, wide monitoring range, low cost and simplicity.[253,254] PEDOT:PSS based CPHs are promising for sensing humidity that depends on water adsorption and desorption by the PSS. On one hand, the insulating and hydrophilic PSS shell is tending to absorb water and swell under high humidity conditions, thus increasing the space between adjacent PEDOT chains, resulting in increased resistivity. On the other hand, low humidity results in water desorbing from the PSS, which reduces the PSS's volume and the space between neighboring PEDOTs, leading to lower resistivity. Nowadays, PEDOT:PSS has been used to develop various types of humidity sensors.[207,255,256] For example, Bian *et al.*[208] developed an interpenetrating PEDOT: PSS based hydrogel humidity sensor with tunable mechanical properties and good conductivity. Thanks to the uniformed conductive component PEDOT:PSS and the hydrogen bonds between water molecules and the large amount of hydrophilic groups in the hydrogel, the obtained CPH humidity sensor exhibited a wide relative humidity range (0–85%).

4.2.3. Other applications

Human–machine interfaces. The interactions of human–machine interfaces are crucial for mobile communications, intelligent robots, and intelligent medical care.[257] Nowadays, increasing interests are considered to develop flexible human–machine interactive devices based on CPHs with their advantages of soft, stretchable and biocompatible performance.[258] Attributing to the ability of CPHs to convert human motion signals into electrical signals, electronic devices such as robots can clearly recognize the commands issued by the human movement and give corresponding feedback. For example, Jing's group[259] developed multifunctional CPHs. Besides fabricating the CPHs as a strain and temperature sensor, the CPHs were assembled as wearable human–machine interface devices, and a smart glove was developed for hand gesture recognition by utilizing the exceptional CPHs, in order to transmit data to a smart phone in real time *via* a bluetooth wireless system.

Implantable electrodes. For implantable electrodes, CPHs must have acceptable biocompatibility, which means that the CPHs must have no major long-term effects *in vivo* or only cause a minor tissue response. For example, when PPy was implanted into the cerebral cortexes of rats, they were tolerated well and allowed the formation of complex neural networks.[260] Nowadays, there are great prospects for using CPHs as implantable devices to monitor human organ motions.[261] For cardiac tissue engineering, Liu and co-workers[262] reported the first functional heart patch that combined conductivity and spontaneous adhesion. The paintable CPHs were synthesized based on polymerizing pyrrole and dopamine in hyperbranched polymer chains. The obtained CPHs could be strongly bonded to the beating heart for 4 weeks, which efficiently boosts the transmission of electrophysiological signals. Consequently, there was a notable improvement in the revascularization of the infarct myocardium and the rebuilding of the cardiac function. Notably, PEDOT:PSS based CPHs possessed both electronic and ionic conductivities with sufficient hydration. On one hand, the CP chains are acting as the charge transfer pathway for electronic carriers. On the other hand, ions are highly mobile in the water-rich hydrophilic polymer matrix.[263] The unique ion/electronic mixed conductivity of PEDOT:PSS based CPHs have been wiedely used as bioelectronic interface for biomedical applications.[264,265]

Flexible energy storage system. CPHs can also be fabricated to work as flexible energy storage devices to power WSs under consecutive stretching, bending and twisting conditions.[266] Principally, CPs inherently bond with the hydrophilic polymer matrix, constructing a continuous conducting and monolithic framework for facilitating the charge transportation. Moreover, an ideal interface between the electrode materials and the electrolyte solution could be established by the porous architectures of the CPHs, promoting a quick and efficient electrochemical reaction.[267] Consequently, CPHs are highly promising for energy storage devices such as supercapacitors and batteries to realize mechanical flexibility, ideal electrochemical performances and additional functions.[268,269] For example, Teng's group[270] reported a high-performance fiber-shaped supercapacitor with a high specific capacitance of 393.8 F cm^{-3} at 2 A cm^{-3} by the *in situ* polymerization of PPy on PEDOT:PSS ECHs. The outstanding electrochemical performance of the fiber shaped ECH supercapacitor can be attributed to the fast electron transfer/ion diffusion and the efficient utilization of the whole electrode, which lead to good electronic and ionic conductor properties, the hierarchically porous structure of the fiber shaped hydrogel and the π–π interaction of the CP network. The rate performance of 52.8% capacitance retention was achieved at a ultrahigh current density of 50 A cm^{-3} probably owing to the hierarchically conductive network and the highly porous interconnected nanostructures in the CPHs, which can accommodate the swelling and shrinking of the polymer network, facilitating the electronic and ionic transfer speed. Mi *et al.*[271] synthesized interconnected CPH coated Si nanoparticles with a reinforced conducting three-dimensional (3D) network structure and used as anode materials for lithium ion batteries. The synergy effect of CPHs enhances the electron transport capability, and results in excellent electrical, mechanical integrity and conductivity of the electrodes.

5. Conclusions and future prospects

In conclusion, the designability of CPHs and their structural closeness to natural soft tissues have sparked a lot of interest in

converting external inputs to electrical signals and monitoring human health in real time. The advantages of CPHs, including high conductivity, tunable mechanical characteristics, self-healing ability, self-adhesiveness, and adequate sensing sensitivity, make them a viable building block for various WSs. In this review, we first present the formation of a molecular network structure, including single component CPHs, CP nanocomposite hydrogels and double-network CPHs. There are mainly two kinds of synthetic processes to construct CPHs, in which CPs either function as conductive fillers or create conductive frameworks. Secondly, the mechanical characteristics, electrical conductivity, and other functionalities vital for WSs (such as self-healing, self-adhesiveness, and biocompatibility) are explored in depth. CPHs have made significant progress in pressure/strain sensors, temperature sensors, and temperature and pressure/strain sensors, thanks to their good electrochemical performance, tunable conductivity, and great mechanical qualities. New prospects and breakthroughs in the fields of medical monitoring and soft robotics will likely result from this recent progress.

Despite the reviewed progress, there is still room for advancements in the field of conductive hydrogels. Due to the fact that most reported CPHs exhibited a nonlinear dependence of sensitivity on low strain, it still remains challenging to obtain linearity, which is crucial for the viability and accuracy of CPH based resistive type WSs. The stress transports from the hydrogel matrix to the conductive network during stretching, and the sensing signal is oriented from the change of the conductive network. The linearity relies on the reliable and continuous conductive network during deformations, which depends on stable and strong interactions between the conductive network and the flexible matrix. To improve the sensing linearity of the CPHs, a possible solution is to eliminate the stiffness difference between CPs and the hydrophilic polymer matrix by constructing chemical and physical chemical bonds between them with excellent affinity. As a result, the conductive pathways and the hydrogels could deform synchronously under strain, leading to a linearly sensing signal.

Another critical issue is the reliability and stability of CPH based WSs in practical applications. The sensing stability of CPHs during long-term operation in a biological environment is a key point for WSs. The evaporation of water would significantly disrupt the electrical conductivity and mechanical performance of CPHs, affecting their sensing functions. Introducing a binary solvent such as glycerin or constructing a hydrophobic organogel to fulfil the CPHs are efficient ways to improve the dehydration feature in the open-air, offering CPHs with long-term sensing stability in extreme environments such as high temperature or cold environments. Taking the appropriately designed CPHs a step further, they could monitor human motion under water without compromising their conductivity and mechanical properties. It is extremely desirable to build specialized structures or incorporate organic agents into CPHs for reliable anti-freezing, long-lasting hydration, and long-term stability qualities. We believe that more trophies are to be collected by developing next generation CPH based WSs, to improve the life quality of human beings.

Conflicts of interest

There are no conflicts to declare.

Acknowledgements

This work was supported partially by the China Postdoctoral Science Foundation (2020M683469), the National Natural Science Foundation of China (No. 22205174 for D. L. and No. 22178278 for F. C.), the Young Talent Support Plan of Xi'an Jiaotong University and the Engineering and Physical Sciences Research Council (EPSRC, UK) grant-EP/N007921. X. Z. acknowledges the support from the NSERC-Alberta Innovated Advanced Program.

References

1 W. Gao, S. Emaminejad, H. Y. Y. Nyein, S. Challa, K. Chen, A. Peck, H. M. Fahad, H. Ota, H. Shiraki, D. Kiriya, D. H. Lien, G. A. Brooks, R. W. Davis and A. Javey, *Nature*, 2016, **529**(7587), 509–514.
2 D. H. Kim, N. Lu, R. Ma, Y. S. Kim, R. H. Kim, S. Wang, J. Wu, S. M. Won, H. Tao, A. Islam, K. J. Yu, T. I. Kim, R. Chowdhury, M. Ying, L. Xu, M. Li, H. J. Chung, H. Keum, M. McCormick, P. Liu, Y. W. Zhang, F. G. Omenetto, Y. Huang, T. Coleman and J. A. Rogers, *Science*, 2011, **333**(6044), 838–843.
3 H. Xu, Y. F. Lu, J. X. Xiang, M. K. Zhang, Y. J. Zhao, Z. Y. Xie and Z. Z. Gu, *Nanoscale*, 2018, **10**(4), 2090–2098.
4 B. An, Y. Ma, W. Li, M. Su, F. Li and Y. Song, *Chem. Commun.*, 2016, **52**(73), 10948–10951.
5 T. Q. Trung, S. Ramasundaram, B. U. Hwang and N. E. Lee, *Adv. Mater.*, 2016, **28**(3), 502–509.
6 L. Song, J. Chen, B. B. Xu and Y. Huang, *ACS Nano*, 2021, **15**(12), 18822–18847.
7 Z. Wang, D. Liu, S. Oleksandr, J. Li, S. K. Arumugam and F. Chen, *Ind. Eng. Chem. Res.*, 2021, **60**(48), 17534–17544.
8 X. Dai, Y. Du, Y. Wang, Y. Liu, N. Xu, Y. Li, D. Shan, B. B. Xu and J. Kong, *ACS Appl. Polym.*, 2020, **2**(3), 1065–1072.
9 Z. Lei, W. Zhu, X. Zhang, X. Wang and P. Wu, *Adv. Funct. Mater.*, 2020, **31**(8), 2008020.
10 W. Zhang, B. Wu, S. Sun and P. Wu, *Nat. Commun.*, 2021, **12**(1), 4082.
11 S. Wang, J. Xu, W. Wang, G. N. Wang, R. Rastak, F. Molina-Lopez, J. W. Chung, S. Niu, V. R. Feig, J. Lopez, T. Lei, S. K. Kwon, Y. Kim, A. M. Foudeh, A. Ehrlich, A. Gasperini, Y. Yun, B. Murmann, J. B. Tok and Z. Bao, *Nature*, 2018, **555**(7694), 83–88.
12 M. Chen, Z. Wang, K. Li, X. Wang and L. Wei, *Adv. Fiber Mater.*, 2021, **3**(1), 1–13.
13 Q. Li, C. Ding, W. Yuan, R. Xie, X. Zhou, Y. Zhao, M. Yu, Z. Yang, J. Sun, Q. Tian, F. Han, H. Li, X. Deng, G. Li and Z. Liu, *Adv. Fiber Mater.*, 2021, **3**(5), 302–311.
14 H. Wei, Z. Wang, H. Zhang, Y. Huang, Z. Wang, Y. Zhou, B. B. Xu, S. Halila and J. Chen, *Chem. Mater.*, 2021, **33**(17), 6731–6742.

15 X. Zhang, N. Sheng, L. Wang, Y. Tan, C. Liu, Y. Xia, Z. Nie and K. Sui, *Mater. Horiz.*, 2019, **6**(2), 326–333.
16 R. Liu, X. Kuang, J. Deng, Y. C. Wang, A. C. Wang, W. Ding, Y. C. Lai, J. Chen, P. Wang, Z. Lin, H. J. Qi, B. Sun and Z. L. Wang, *Adv. Mater.*, 2018, **30**(8), 1705195.
17 J. Y. Sun, C. Keplinger, G. M. Whitesides and Z. Suo, *Adv. Mater.*, 2014, **26**(45), 7608–7614.
18 Y. J. Liu, W. T. Cao, M. G. Ma and P. Wan, *ACS Appl. Mater. Interfaces*, 2017, **9**(30), 25559–25570.
19 H. Ouyang, J. Tian, G. Sun, Y. Zou, Z. Liu, H. Li, L. Zhao, B. Shi, Y. Fan, Y. Fan, Z. L. Wang and Z. Li, *Adv. Mater.*, 2017, **29**(40), 1703456.
20 T. Yang, X. Jiang, Y. Zhong, X. Zhao, S. Lin, J. Li, X. Li, J. Xu, Z. Li and H. Zhu, *ACS Sens.*, 2017, **2**(7), 967–974.
21 N. Luo, W. Dai, C. Li, Z. Zhou, L. Lu, C. C. Y. Poon, S.-C. Chen, Y. Zhang and N. Zhao, *Adv. Funct. Mater.*, 2016, **26**(8), 1178–1187.
22 G. Ge, Y. Lu, X. Qu, W. Zhao, Y. Ren, W. Wang, Q. Wang, W. Huang and X. Dong, *ACS Nano*, 2020, **14**(1), 218–228.
23 V. P. Rachim and W.-Y. Chung, *Sens. Actuators, B*, 2019, **286**, 173–180.
24 S. H. Kim, S. Jung, I. S. Yoon, C. Lee, Y. Oh and J.-M. Hong, *Adv. Mater.*, 2018, **30**(26), 1800109.
25 H. Ding, X. Liang, Q. Wang, M. Wang, Z. Li and G. Sun, *Carbohydr. Polym.*, 2020, **248**, 116797.
26 L. Sun, H. Huang, Q. Ding, Y. Guo, W. Sun, Z. Wu, M. Qin, Q. Guan and Z. You, *Adv. Fiber Mater.*, 2021, **4**(1), 98–107.
27 Z. Wang, H. Zhou, D. Liu, X. Chen, D. Wang, S. Dai, F. Chen and B. B. Xu, *Adv. Funct. Mater.*, 2022, **32**(25), 2201396.
28 Q. Peng, J. Chen, T. Wang, X. Peng, J. Liu, X. Wang, J. Wang and H. Zeng, *InfoMat*, 2020, **2**(5), 843–865.
29 M. Ju, B. Wu, S. Sun and P. Wu, *Adv. Funct. Mater.*, 2020, **30**(14), 1910387.
30 J. Zhang, Q. Zhang, X. Liu, S. Xia, Y. Gao and G. Gao, *J. Polym. Sci.*, 2022, **60**(18), 2663–2678.
31 T. Ye, J. Wang, Y. Jiao, L. Li, E. He, L. Wang, Y. Li, Y. Yun, D. Li, J. Lu, H. Chen, Q. Li, F. Li, R. Gao, H. Peng and Y. Zhang, *Adv. Mater.*, 2022, **34**(4), e2105120.
32 Z. Shen, Z. Zhang, N. Zhang, J. Li, P. Zhou, F. Hu, Y. Rong, B. Lu and G. Gu, *Adv. Mater.*, 2022, **34**(32), e2203650.
33 J. Lei, Z. Li, S. Xu and Z. Liu, *Acta Mech. Sin.*, 2021, **37**(3), 367–386.
34 J. Wang, Y. Du, J. Wang, W. Gong, L. Xu, L. Yan, Y. You, W. Lu and X. Zhang, *Langmuir*, 2021, **37**(19), 5923–5931.
35 X. Liang, G. Chen, S. Lin, J. Zhang, L. Wang, P. Zhang, Z. Wang, Z. Wang, Y. Lan, Q. Ge and J. Liu, *Adv. Mater.*, 2021, **33**(30), e2102011.
36 X. Liang, G. Chen, I. M. Lei, P. Zhang, Z. Wang, X. Chen, M. Lu, J. Zhang, Z. Wang, T. Sun, Y. Lan and J. Liu, *Adv. Mater.*, 2022, e2207587.
37 D. N. Heo, N. J. Castro, S. J. Lee, H. Noh, W. Zhu and L. G. Zhang, *Nanoscale*, 2017, **9**(16), 5055–5062.
38 H. Yan, J. Zhou, C. Wang, H. Gong, W. Liu, W. Cen, G. Yuan and Y. Long, *Smart Mater. Struct.*, 2021, **31**(1), 015019.
39 B. Lu, H. Yuk, S. Lin, N. Jian, K. Qu, J. Xu and X. Zhao, *Nat. Commun.*, 2019, **10**(1), 1043.
40 N. Dianat, M. S. Rahmanifar, A. Noori, M. F. El-Kady, X. Chang, R. B. Kaner and M. F. Mousavi, *Nano Lett.*, 2021, **21**(22), 9485–9493.
41 J. Tong, C. Han, X. Hao, X. Qin and B. Li, *ACS Appl. Mater. Interfaces*, 2020, **12**(35), 39630–39638.
42 C. Huyan, S. Ding, Z. Lyu, M. H. Engelhard, Y. Tian, D. Du, D. Liu and Y. Lin, *ACS Appl. Mater. Interfaces*, 2021, **13**(41), 48500–48507.
43 S. Ding, Z. Lyu, L. Fang, T. Li, W. Zhu, S. Li, X. Li, J. C. Li, D. Du and Y. Lin, *Small*, 2021, **17**(25), e2100664.
44 M. A. Bhat, R. A. Rather and A. H. Shalla, *Synth. Met.*, 2021, **273**, 116709.
45 J. Zhang, L. Wang, Y. Xue, I. M. Lei, X. Chen, P. Zhang, C. Cai, X. Liang, Y. Lu and J. Liu, *Adv. Mater.*, 2022, e2209324.
46 G. Kaur, R. Adhikari, P. Cass, M. Bown and P. Gunatillake, *RSC Adv.*, 2015, **5**(47), 37553–37567.
47 X. Guo and A. Facchetti, *Nat. Mater.*, 2020, **19**(9), 922–928.
48 T. Nezakati, A. Seifalian, A. Tan and A. M. Seifalian, *Chem. Rev.*, 2018, **118**(14), 6766–6843.
49 Z. Zhao, K. Xia, Y. Hou, Q. Zhang, Z. Ye and J. Lu, *Chem. Soc. Rev.*, 2021, **50**(22), 12702–12743.
50 K. Haraguchi and H. J. Li, *Angew. Chem., Int. Ed.*, 2005, **44**(40), 6500–6504.
51 C. Hu, Y. Zhang, X. Wang, L. Xing, L. Shi and R. Ran, *ACS Appl. Mater. Interfaces*, 2018, **10**(50), 44000–44010.
52 L. Li, Y. Wang, L. Pan, Y. Shi, W. Cheng, Y. Shi and G. Yu, *Nano Lett.*, 2015, **15**(2), 1146–1151.
53 R. Wu, L. Li, L. Pan, K. Yan, Y. Shi, L. Jiang and J. J. Zhu, *J. Mater. Chem. B*, 2021, **9**(46), 9514–9523.
54 Z. Wang, J. Chen, Y. Cong, H. Zhang, T. Xu, L. Nie and J. Fu, *Chem. Mater.*, 2018, **30**(21), 8062–8069.
55 L. Pan, G. Yu, D. Zhai, H. R. Lee, W. Zhao, N. Liu, H. Wang, B. C.-K. Tee, Y. Shi, Y. Cui and Z. Bao, *Proc. Natl. Acad. Sci. U. S. A.*, 2012, **109**(24), 9287–9292.
56 Q. Ding, X. Xu, Y. Yue, C. Mei, C. Huang, S. Jiang, Q. Wu and J. Han, *ACS Appl. Mater. Interfaces*, 2018, **10**(33), 27987–28002.
57 M. S. Ting, J. Travas-Sejdic and J. Malmstrom, *J. Mater. Chem. B*, 2021, **9**(37), 7578–7596.
58 Y. Z. Zhang, K. H. Lee, D. H. Anjum, R. Sougrat, Q. Jiang, H. Kim and H. N. Alshareef, *Sci. Adv.*, 2018, **4**(6), eaat0098.
59 B. Xing, C. W. Yu, K. H. Chow, P. L. Ho, D. Fu and B. Xu, *J. Am. Chem. Soc.*, 2002, **124**(50), 14846–14847.
60 K. Zhang, X. Chen, Y. Xue, J. Lin, X. Liang, J. Zhang, J. Zhang, G. Chen, C. Cai and J. Liu, *Adv. Funct. Mater.*, 2021, **32**(15), 2111465.
61 O. Wichterle and D. Lím, *Nature*, 1960, **185**(4706), 117–118.
62 E. M. Ahmed, *J. Adv. Res.*, 2015, **6**(2), 105–121.
63 D. A. Ossipov and J. Hilborn, *Macromolecules*, 2006, **39**(5), 1709–1718.
64 Z. Wu, X. Yang and J. Wu, *ACS Appl. Mater. Interfaces*, 2021, **13**(2), 2128–2144.
65 C. Yang and Z. Suo, *Nat. Rev. Mater.*, 2018, **3**(6), 125–142.

66 B. Yao, H. Wang, Q. Zhou, M. Wu, M. Zhang, C. Li and G. Shi, *Adv. Mater.*, 2017, **29**(28), 1700974.
67 T. Cheng, Y. Z. Zhang, S. Wang, Y. L. Chen, S. Y. Gao, F. Wang, W. Y. Lai and W. Huang, *Adv. Funct. Mater.*, 2021, **31**(24), 2101303.
68 P. Tan, H. Wang, F. Xiao, X. Lu, W. Shang, X. Deng, H. Song, Z. Xu, J. Cao, T. Gan, B. Wang and X. Zhou, *Nat. Commun.*, 2022, **13**(1), 358.
69 V. Garg, T. Gupta, S. Rani, S. Bandyopadhyay-Ghosh, S. B. Ghosh, L. Qiao and G. Liu, *Compos. Sci. Technol.*, 2021, **213**, 108894.
70 F. Fu, J. Wang, H. Zeng and J. Yu, *ACS Mater. Lett.*, 2020, **2**(10), 1287–1301.
71 S. Hasan, A. Z. Kouzani, S. Adams, J. Long and M. A. P. Mahmud, *Sens. Actuators, A*, 2022, **335**, 113382.
72 X. Sun, F. Yao and J. Li, *J. Mater. Chem. A*, 2020, **8**(36), 18605–18623.
73 J. Kim, J. Lee, J. You, M.-S. Park, M. S. A. Hossain, Y. Yamauchi and J. H. Kim, *Mater. Horiz.*, 2016, **3**(6), 517–535.
74 Y. Wang, Y. Ding, X. Guo and G. Yu, *Nano Res.*, 2019, **12**(9), 1978–1987.
75 P. Chakraborty, T. Guterman, N. Adadi, M. Yadid, T. Brosh, L. Adler-Abramovich, T. Dvir and E. Gazit, *ACS Nano*, 2019, **13**(1), 163–175.
76 L. Han, H. Zhang, H. Y. Yu, Z. Ouyang, J. Yao, I. Krucinska, D. Kim and K. C. Tam, *Biosens. Bioelectron.*, 2021, **191**, 113467.
77 H. Wei, D. Kong, T. Li, Q. Xue, S. Wang, D. Cui, Y. Huang, L. Wang, S. Hu, T. Wan and G. Yang, *ACS Sens.*, 2021, **6**(8), 2938–2951.
78 J. Chen, Q. Peng, T. Thundat and H. Zeng, *Chem. Mater.*, 2019, **31**(12), 4553–4563.
79 D. Zhang, J. Jian, Y. Xie, S. Gao, Z. Ling, C. Lai, J. Wang, C. Wang, F. Chu and M.-J. Dumont, *Chem. Eng. J.*, 2022, **427**, 130921.
80 J. Wang, Y. Lin, A. Mohamed, Q. Ji and H. Jia, *J. Mater. Chem. C*, 2021, **9**(2), 575–583.
81 X. Sun, W. Zhong, Z. Zhang, H. Liao and C. Zhang, *J. Mater. Sci.*, 2022, **57**(26), 12511–12521.
82 J. Cong, Z. Fan, S. Pan, J. Tian, W. Lian, S. Li, S. Wang, D. Zheng, C. Miao, W. Ding, T. Sun and T. Luo, *ACS Appl. Mater. Interfaces*, 2021, **13**(29), 34942–34953.
83 D. Gan, L. Han, M. Wang, W. Xing, T. Xu, H. Zhang, K. Wang, L. Fang and X. Lu, *ACS Appl. Mater. Interfaces*, 2018, **10**(42), 36218–36228.
84 D. Liu, H. Zhou, Y. Zhao, C. Huyan, Z. Wang, H. Torun, Z. Guo, S. Dai, B. B. Xu and F. Chen, *Small*, 2022, e2203258.
85 D. Gan, T. Shuai, X. Wang, Z. Huang, F. Ren, L. Fang, K. Wang, C. Xie and X. Lu, *Nanomicro Lett.*, 2020, **12**(1), 169.
86 X. Sun, H. Wang, Y. Ding, Y. Yao, Y. Liu and J. Tang, *J. Mater. Chem. B*, 2022, **10**(9), 1442–1452.
87 Y. Li, Q. Gong, X. Liu, Z. Xia, Y. Yang, C. Chen and C. Qian, *Carbohydr. Polym.*, 2021, **267**, 118207.
88 Z. Ma, W. Shi, K. Yan, L. Pan and G. Yu, *Chem. Sci.*, 2019, **10**(25), 6232–6244.
89 L. Han, L. Yan, M. Wang, K. Wang, L. Fang, J. Zhou, J. Fang, F. Ren and X. Lu, *Chem. Mater.*, 2018, **30**(16), 5561–5572.
90 X. Yu, H. Zhang, Y. Wang, X. Fan, Z. Li, X. Zhang and T. Liu, *Adv. Funct. Mater.*, 2022, **32**(33), 2204366.
91 Y. Wang, Y. Shi, L. Pan, Y. Ding, Y. Zhao, Y. Li, Y. Shi and G. Yu, *Nano Lett.*, 2015, **15**(11), 7736–7741.
92 P. Dou, Z. Liu, Z. Cao, J. Zheng, C. Wang and X. Xu, *J. Mater. Sci.*, 2016, **51**(9), 4274–4282.
93 L. Zhou, L. Fan, X. Yi, Z. Zhou, C. Liu, R. Fu, C. Dai, Z. Wang, X. Chen, P. Yu, D. Chen, G. Tan, Q. Wang and C. Ning, *ACS Nano*, 2018, **12**(11), 10957–10967.
94 Q. Wu, J. Wei, B. Xu, X. Liu, H. Wang, W. Wang, Q. Wang and W. Liu, *Sci. Rep.*, 2017, **7**, 41566.
95 Y. Y. Lee, H. Y. Kang, S. H. Gwon, G. M. Choi, S. M. Lim, J. Y. Sun and Y. C. Joo, *Adv. Mater.*, 2016, **28**(8), 1636–1643.
96 S. Rani, T. Gupta, V. Garg, S. Bandyopadhyay-Ghosh, S. Bandhu Ghosh and G. Liu, *Mater. Today Proc.*, 2022, **62**, 638–643.
97 C. Li, *RSC Adv.*, 2021, **11**(54), 33835–33848.
98 M. Moussa, M. F. El-Kady, D. Dubal, T. T. Tung, M. J. Nine, N. Mohamed, R. B. Kaner and D. Losic, *ACS Appl. Energy Mater.*, 2019, **3**(1), 923–932.
99 Y. Zhao, B. Zhang, B. Yao, Y. Qiu, Z. Peng, Y. Zhang, Y. Alsaid, I. Frenkel, K. Youssef, Q. Pei and X. He, *Matter*, 2020, **3**(4), 1196–1210.
100 L. V. Kayser and D. J. Lipomi, *Adv. Mater.*, 2019, **31**(10), e1806133.
101 X. Ren, M. Yang, T. Yang, C. Xu, Y. Ye, X. Wu, X. Zheng, B. Wang, Y. Wan and Z. Luo, *ACS Appl. Mater. Interfaces*, 2021, **13**(21), 25374–25382.
102 S. Choi, S. I. Han, D. Kim, T. Hyeon and D. H. Kim, *Chem. Soc. Rev.*, 2019, **48**(6), 1566–1595.
103 H. Pang, L. Xu, D.-X. Yan and Z.-M. Li, *Prog. Polym. Sci.*, 2014, **39**(11), 1908–1933.
104 F. O. Obiweluozor, B. Maharjan, A. Gladys Emechebe, C. H. Park and C. S. Kim, *Chem. Eng. J*, 2018, **347**, 932–943.
105 S. Lv, J. Nie, Q. Gao, C. Xie, L. Zhou, J. Qiu, J. Fu, X. Zhao and Y. He, *Biofabrication*, 2020, **12**(2), 025015.
106 A. Paikar, A. I. Novichkov, A. I. Hanopolskyi, V. A. Smaliak, X. Sui, N. Kampf, E. V. Skorb and S. N. Semenov, *Adv. Mater.*, 2022, **34**(13), e2106816.
107 Z. Qiu, Z. Wu, M. Zhong, M. Yang, J. Xu, G. Zhang, Z. Qin and B. R. Yang, *Adv. Mater. Technol.*, 2021, **7**(5), 2100961.
108 H. Liu, M. Li, C. Ouyang, T. J. Lu, F. Li and F. Xu, *Small*, 2018, **14**(36), e1801711.
109 S. Ma, S. Wang, Q. Li, Y. Leng, L. Wang and G.-H. Hu, *Ind. Eng. Chem. Res.*, 2017, **56**(28), 7971–7976.
110 K. Peng, L. K. Vora, J. Dominguez-Robles, Y. A. Naser, M. Li, E. Larraneta and R. F. Donnelly, *Mater. Sci. Eng., C*, 2021, **127**, 112226.
111 M. Wang, H. Zhou, H. Du, L. Chen, G. Zhao, H. Liu, X. Jin, W. Chen and A. Ma, *Chem. Eng. J.*, 2022, **446**, 137163.
112 Y. Ma, Y. Gao, L. Liu, X. Ren and G. Gao, *Chem. Mater.*, 2020, **32**(20), 8938–8946.
113 H. Zhou, M. Wang, X. Jin, H. Liu, J. Lai, H. Du, W. Chen and A. Ma, *ACS Appl. Mater. Interfaces*, 2021, **13**(1), 1441–1451.

114 R. Yang, X. Chen, Y. Zheng, K. Chen, W. Zeng and X. Wu, *J. Mater. Chem. C*, 2022, **10**(14), 5380–5399.
115 H. Li, C. Tan and L. Li, *Mater. Design*, 2018, **159**, 20–38.
116 Z. Chen, D. Zhao, B. Liu, G. Nian, X. Li, J. Yin, S. Qu and W. Yang, *Adv. Funct. Mater.*, 2019, **29**(20), 1900971.
117 R. S. Jordan, J. Frye, V. Hernandez, I. Prado, A. Giglio, N. Abbasizadeh, M. Flores-Martinez, K. Shirzad, B. Xu, I. M. Hill and Y. Wang, *J. Mater. Chem. B*, 2021, **9**(35), 7258–7270.
118 C. Loebel, C. B. Rodell, M. H. Chen and J. A. Burdick, *Nat. Protoc.*, 2017, **12**(8), 1521–1541.
119 H. Yuk, B. Lu, S. Lin, K. Qu, J. Xu, J. Luo and X. Zhao, *Nat. Commun.*, 2020, **11**(1), 1604.
120 M. Yue, Y. Wang, H. Guo, C. Zhang and T. Liu, *Compos. Sci. Technol.*, 2022, **220**, 109263.
121 E. Fantino, I. Roppolo, D. Zhang, J. Xiao, A. Chiappone, M. Castellino, Q. Guo, C. F. Pirri and J. Yang, *Macromol. Mater. Eng.*, 2018, **303**(4), 1700356.
122 Z. Yang, J. Ma, B. Bai, A. Qiu, D. Losic, D. Shi and M. Chen, *Electrochim. Acta*, 2019, **322**, 134769.
123 D. W. Kim, J. H. Lee, J. K. Kim and U. Jeong, *NPG Asia Mater.*, 2020, **12**(1), 6.
124 M. Wang, Q. Gao, J. Gao, C. Zhu and K. Chen, *J. Mater. Chem. C*, 2020, **8**(13), 4564–4571.
125 Z. Wang, Y. Cong and J. Fu, *J. Mater. Chem. B*, 2020, **8**(16), 3437–3459.
126 Z. Tao, H. Fan, J. Huang, T. Sun, T. Kurokawa and J. P. Gong, *ACS Appl. Mater. Interfaces*, 2019, **11**(40), 37139–37146.
127 D. Mawad, E. Stewart, D. L. Officer, T. Romeo, P. Wagner, K. Wagner and G. G. Wallace, *Adv. Funct. Mater.*, 2012, **22**(13), 2692–2699.
128 K. A. Milakin, Z. Morávková, U. Acharya, M. Kašparová, S. Breitenbach, O. Taboubi, J. Hodan, J. Hromádková, C. Unterweger, P. Humpolíček and P. Bober, *Polymer*, 2021, 217.
129 Y. Lu, W. He, T. Cao, H. Guo, Y. Zhang, Q. Li, Z. Shao, Y. Cui and X. Zhang, *Sci. Rep.*, 2014, **4**, 5792.
130 P. Li, Z. Jin, L. Peng, F. Zhao, D. Xiao, Y. Jin and G. Yu, *Adv. Mater.*, 2018, **30**(18), 1800124.
131 C. Rinoldi, M. Lanzi, R. Fiorelli, P. Nakielski, K. Zembrzycki, T. Kowalewski, O. Urbanek, V. Grippo, K. Jezierska-Wozniak, W. Maksymowicz, A. Camposeo, R. Bilewicz, D. Pisignano, N. Sanai and F. Pierini, *Biomacromolecules*, 2021, **22**(7), 3084–3098.
132 Q. Rong, W. Lei and M. Liu, *Chemistry*, 2018, **24**(64), 16930–16943.
133 G. Su, S. Yin, Y. Guo, F. Zhao, Q. Guo, X. Zhang, T. Zhou and G. Yu, *Mater. Horiz.*, 2021, **8**(6), 1795–1804.
134 Y. Peng, M. Pi, X. Zhang, B. Yan, Y. Li, L. Shi and R. Ran, *Polymer*, 2020, **196**, 122469.
135 Y. Li, C. Liu, X. Lv and S. Sun, *Soft Matter*, 2021, **17**(8), 2142–2150.
136 S. Cao, X. Tong, K. Dai and Q. Xu, *J. Mater. Chem. A*, 2019, **7**(14), 8204–8209.
137 Y. Geng, X. Y. Lin, P. Pan, G. Shan, Y. Bao, Y. Song, Z. L. Wu and Q. Zheng, *Polymer*, 2016, **100**, 60–68.
138 F. Lü, S. Zhao, R. Guo, J. He, X. Peng, H. Bao, J. Fu, L. Han, G. Qi, J. Luo, X. Tang and X. Liu, *Nano Energy*, 2019, **61**, 420–427.
139 V. R. Feig, H. Tran, M. Lee, K. Liu, Z. Huang, L. Beker, D. G. Mackanic and Z. Bao, *Adv. Mater.*, 2019, **31**(39), e1902869.
140 Y. Xu, X. Yang, A. K. Thomas, P. A. Patsis, T. Kurth, M. Krater, K. Eckert, M. Bornhauser and Y. Zhang, *ACS Appl. Mater. Interfaces*, 2018, **10**(17), 14418–14425.
141 S. Peng, Y. Yu, S. Wu and C. H. Wang, *ACS Appl. Mater. Interfaces*, 2021, **13**(37), 43831–43854.
142 Y. Zou, C. Chen, Y. Sun, S. Gan, L. Dong, J. Zhao and J. Rong, *Chem. Eng. J.*, 2021, **418**, 128616.
143 D. Wu and W. Zhong, *J. Mater. Chem. A*, 2019, **7**(10), 5819–5830.
144 H. H. Hsu, X. Zhang, K. Xu, Y. Wang, Q. Wang, G. Luo, M. Xing and W. Zhong, *Chem. Eng. J.*, 2021, 422.
145 M. Zhong, Y. T. Liu, X. Y. Liu, F. K. Shi, L. Q. Zhang, M. F. Zhu and X. M. Xie, *Soft Matter*, 2016, **12**(24), 5420–5428.
146 H. Liu, X. Wang, Y. Cao, Y. Yang, Y. Yang, Y. Gao, Z. Ma, J. Wang, W. Wang and D. Wu, *ACS Appl. Mater. Interfaces*, 2020, **12**(22), 25334–25344.
147 Y. Shi, C. Ma, L. Peng and G. Yu, *Adv. Funct. Mater.*, 2015, **25**(8), 1219–1225.
148 Z. Wang, H. Zhou, J. Lai, B. Yan, H. Liu, X. Jin, A. Ma, G. Zhang, W. Zhao and W. Chen, *J. Mater. Chem. C*, 2018, **6**(34), 9200–9207.
149 Z. Wang, H. Zhou, W. Chen, Q. Li, B. Yan, X. Jin, A. Ma, H. Liu and W. Zhao, *ACS Appl. Mater. Interfaces*, 2018, **10**(16), 14045–14054.
150 S. Hu, L. Zhou, L. Tu, C. Dai, L. Fan, K. Zhang, T. Yao, J. Chen, Z. Wang, J. Xing, R. Fu, P. Yu, G. Tan, J. Du and C. Ning, *J. Mater. Chem. B*, 2019, **7**(15), 2389–2397.
151 X. Jin, H. Jiang, G. Li, B. Fu, X. Bao, Z. Wang and Q. Hu, *Chem. Eng. J.*, 2020, **394**, 124901.
152 Q. Yan, M. Zhou and H. Fu, *Composites, Part B*, 2020, 201.
153 M. Song, H. Yu, J. Zhu, Z. Ouyang, S. Y. H. Abdalkarim, K. C. Tam and Y. Li, *Chem. Eng. J.*, 2020, 398.
154 W. Li, F. Gao, X. Wang, N. Zhang and M. Ma, *Angew. Chem., Int. Ed.*, 2016, **55**(32), 9196–9201.
155 Y. Li, Q. Gong, L. Han, X. Liu, Y. Yang, C. Chen, C. Qian and Q. Han, *Carbohydr. Polym.*, 2022, **298**, 120060.
156 M. Wang, H. Zhou, X. Jin, H. Liu, A. Ma, H. Yan, L. Chen and W. Chen, *J. Mater. Chem. C*, 2021, **9**(5), 1822–1828.
157 A. Shit, S. B. Heo, I. In and S. Y. Park, *ACS Appl. Mater. Interfaces*, 2020, **12**(30), 34105–34114.
158 X. Han, G. Xiao, Y. Wang, X. Chen, G. Duan, Y. Wu, X. Gong and H. Wang, *J. Mater. Chem. A*, 2020, **8**(44), 23059–23095.
159 Z. Chen, Y. Chen, M. S. Hedenqvist, C. Chen, C. Cai, H. Li, H. Liu and J. Fu, *J. Mater. Chem. B*, 2021, **9**(11), 2561–2583.
160 H. Zhang, H. Shen, J. Lan, H. Wu, L. Wang and J. Zhou, *Carbohydr. Polym.*, 2022, **295**, 119848.
161 X. Liu, X. Chen, X. Chi, Z. Feng, C. Yang, R. Gao, S. Li, C. Zhang, X. Chen, P. Huang, A. Dong, D. Kong and W. Wang, *Nano Energy*, 2022, **92**, 106735.

162 X. Liang, G. Chen, S. Lin, J. Zhang, L. Wang, P. Zhang, Y. Lan and J. Liu, *Adv. Mater.*, 2022, **34**(8), e2107106.
163 Y. Zhao, Z. Li, S. Song, K. Yang, H. Liu, Z. Yang, J. Wang, B. Yang and Q. Lin, *Adv. Funct. Mater.*, 2019, **29**(31), 1901474.
164 J. P. Gong, Y. Katsuyama, T. Kurokawa and Y. Osada, *Adv. Mater.*, 2003, **15**(14), 1155–1158.
165 H. Sun, Y. Zhao, C. Wang, K. Zhou, C. Yan, G. Zheng, J. Huang, K. Dai, C. Liu and C. Shen, *Nano Energy*, 2020, 76.
166 X. Zhao, *Soft Matter*, 2014, **10**(5), 672–687.
167 Y. Xu, P. A. Patsis, S. Hauser, D. Voigt, R. Rothe, M. Gunther, M. Cui, X. Yang, R. Wieduwild, K. Eckert, C. Neinhuis, T. F. Akbar, I. R. Minev, J. Pietzsch and Y. Zhang, *Adv. Sci.*, 2019, **6**(15), 1802077.
168 K. X. Hou, S. P. Zhao, D. P. Wang, P. C. Zhao, C. H. Li and J. L. Zuo, *Adv. Funct. Mater.*, 2021, **31**(49), 2107006.
169 G. Wu, K. Jin, L. Liu and H. Zhang, *Soft Matter*, 2020, **16**(13), 3319–3324.
170 M. Wu, J. Chen, Y. Ma, B. Yan, M. Pan, Q. Peng, W. Wang, L. Han, J. Liu and H. Zeng, *J. Mater. Chem. A*, 2020, **8**(46), 24718–24733.
171 X. Sun, F. Yao, C. Wang, Z. Qin, H. Zhang, Q. Yu, H. Zhang, X. Dong, Y. Wei and J. Li, *Macromol. Rapid Commun.*, 2020, **41**(13), 2000185.
172 Y. Jiao, Y. Lu, K. Lu, Y. Yue, X. Xu, H. Xiao, J. Li and J. Han, *J. Colloid Interface Sci.*, 2021, **597**, 171–181.
173 S. Liu and L. Li, *ACS Appl. Mater. Interfaces*, 2017, **9**(31), 26429–26437.
174 K. Pan, S. Peng, Y. Chu, K. Liang, C. H. Wang, S. Wu and J. Xu, *J. Polym. Sci.*, 2020, **58**(21), 3069–3081.
175 J. Zhao, G. Ji, Y. Li, R. Hu and J. Zheng, *Chem. Eng. J.*, 2021, **420**, 129790.
176 Y. Fang, J. Xu, F. Gao, X. Du, Z. Du, X. Cheng and H. Wang, *Composites, Part B*, 2021, **219**, 108965.
177 S. Liu, R. Zheng, S. Chen, Y. Wu, H. Liu, P. Wang, Z. Deng and L. Liu, *J. Mater. Chem. C*, 2018, **6**(15), 4183–4190.
178 N. Zheng, Y. Xu, Q. Zhao and T. Xie, *Chem. Rev.*, 2021, **121**(3), 1716–1745.
179 G. Zhang, S. Chen, Z. Peng, W. Shi, Z. Liu, H. Shi, K. Luo, G. Wei, H. Mo, B. Li and L. Liu, *ACS Appl. Mater. Interfaces*, 2021, **13**(10), 12531–12540.
180 C. Xie, X. Wang, H. He, Y. Ding and X. Lu, *Adv. Funct. Mater.*, 2020, **30**(25), 1909954.
181 Y. Xue, J. Zhang, X. Chen, J. Zhang, G. Chen, K. Zhang, J. Lin, C. Guo and J. Liu, *Adv. Funct. Mater.*, 2021, **31**(47), 2106446.
182 Z. Zhang, Z. Gao, Y. Wang, L. Guo, C. Yin, X. Zhang, J. Hao, G. Zhang and L. Chen, *Macromolecules*, 2019, **52**(6), 2531–2541.
183 Y. Zhang, K. Chen, Y. Li, J. Lan, B. Yan, L. Shi and R. Ran, *ACS Appl. Mater. Interfaces*, 2019, **11**(50), 47350–47357.
184 A. H. Hofman, I. A. van Hees, J. Yang and M. Kamperman, *Adv. Mater.*, 2018, **30**(19), e1704640.
185 X. Chen, J. Zhang, G. Chen, Y. Xue, J. Zhang, X. Liang, I. M. Lei, J. Lin, B. B. Xu and J. Liu, *Adv. Funct. Mater.*, 2022, **32**(29), 2202285.
186 X. Liu, Q. Zhang, L. Duan and G. Gao, *Adv. Funct. Mater.*, 2019, **29**(17), 1900450.
187 C. Liu, Z. Cai, Y. Zhao, H. Zhao and F. Ge, *Cellulose*, 2015, **23**(1), 637–648.
188 G. Li, C. Li, G. Li, D. Yu, Z. Song, H. Wang, X. Liu, H. Liu and W. Liu, *Small*, 2022, **18**(5), e2101518.
189 Q. Wang, X. Pan, C. Lin, D. Lin, Y. Ni, L. Chen, L. Huang, S. Cao and X. Ma, *Chem. Eng. J.*, 2019, **370**, 1039–1047.
190 X. Zhao, H. Wu, B. Guo, R. Dong, Y. Qiu and P. X. Ma, *Biomaterials*, 2017, **122**, 34–47.
191 A. Sivashanmugam, R. Arun Kumar, M. Vishnu Priya, S. V. Nair and R. Jayakumar, *Eur. Polym. J.*, 2015, **72**, 543–565.
192 W. Zhao, D. Zhang, Y. Yang, C. Du and B. Zhang, *J. Mater. Chem. A*, 2021, **9**(38), 22082–22094.
193 M. Amjadi, K.-U. Kyung, I. Park and M. Sitti, *Adv. Funct. Mater.*, 2016, **26**(11), 1678–1698.
194 H. Yuk, B. Lu and X. Zhao, *Chem. Soc. Rev.*, 2019, **48**(6), 1642–1667.
195 D. Zhang, Y. Tang, Y. Zhang, F. Yang, Y. Liu, X. Wang, J. Yang, X. Gong and J. Zheng, *J. Mater. Chem. A*, 2020, **8**(39), 20474–20485.
196 F. Ye, M. Li, D. Ke, L. Wang and Y. Lu, *Adv. Mater. Technol.*, 2019, **4**(9), 1900346.
197 J. C. Yang, J. Mun, S. Y. Kwon, S. Park, Z. Bao and S. Park, *Adv. Mater.*, 2019, **31**(48), e1904765.
198 Y. Wang, Q. Chang, R. Zhan, K. Xu, Y. Wang, X. Zhang, B. Li, G. Luo, M. Xing and W. Zhong, *J. Mater. Chem. A*, 2019, **7**(43), 24814–24829.
199 F. Zhao, Y. Shi, L. Pan and G. Yu, *Acc. Chem. Res.*, 2017, **50**(7), 1734–1743.
200 S. Raman and A. Ravi Sankar, *J. Mater. Sci.*, 2022, **57**(28), 13152–13178.
201 K. Zhai, H. Wang, Q. Ding, Z. Wu, M. Ding, K. Tao, B. R. Yang, X. Xie, C. Li and J. Wu, *Adv. Sci.*, 2023, **10**(6), e2205632.
202 J. Wu, W. Huang, Z. Wu, X. Yang, A. G. P. Kottapalli, X. Xie, Y. Zhou and K. Tao, *ACS Mater. Lett.*, 2022, **4**(9), 1616–1629.
203 H. Liu, Q. Li, S. Zhang, R. Yin, X. Liu, Y. He, K. Dai, C. Shan, J. Guo, C. Liu, C. Shen, X. Wang, N. Wang, Z. Wang, R. Wei and Z. Guo, *J. Mater. Chem. C*, 2018, **6**(45), 12121–12141.
204 Z. Jia, G. Li, J. Wang, S. Su, J. Wen, J. Yuan, M. Pan and Z. Pan, *New J. Chem.*, 2021, **45**(16), 7321–7331.
205 T. Zhan, H. Xie, J. Mao, S. Wang, Y. Hu and Z. Guo, *ChemistrySelect*, 2021, **6**(17), 4229–4237.
206 G. Su, Y. Zhang, X. Zhang, J. Feng, J. Cao, X. Zhang and T. Zhou, *Chem. Mater.*, 2022, **34**(3), 1392–1402.
207 F. Hossein-Babaei, T. Akbari and B. Harkinezhad, *Sens. Actuators, B*, 2019, **293**, 329–335.
208 Z. Bian, Y. Li, H. Sun, M. Shi, Y. Zheng, H. Liu, C. Liu and C. Shen, *Carbohydr. Polym.*, 2023, **301**, 120300.
209 L. Wang, H. Huang, S. Xiao, D. Cai, Y. Liu, B. Liu, D. Wang, C. Wang, H. Li, Y. Wang, Q. Li and T. Wang, *ACS Appl. Mater. Interfaces*, 2014, **6**(16), 14131–14140.

210 M. Serafini, F. Mariani, I. Gualandi, F. Decataldo, L. Possanzini, M. Tessarolo, B. Fraboni, D. Tonelli and E. Scavetta, *Sensors*, 2021, **21**(23), 7905.
211 F. Decataldo, F. Bonafe, F. Mariani, M. Serafini, M. Tessarolo, I. Gualandi, E. Scavetta and B. Fraboni, *Polymers*, 2022, **14**(5), 1022.
212 J. J. Alcaraz-Espinoza, G. Ramos-Sánchez, J. H. Sierra-Uribe and I. González, *ACS Appl. Energy Mater.*, 2021, **4**(9), 9099–9110.
213 Q. Chen, H. Lu, F. Chen, L. Chen, N. Zhang and M. Ma, *ACS Appl. Energy Mater.*, 2018, **1**(8), 4261–4268.
214 J. Yang, J. Luo, H. Liu, L. Shi, K. Welch, Z. Wang and M. Strømme, *Ind. Eng. Chem. Res.*, 2020, **59**(19), 9310–9317.
215 D. D. L. Chung, *J. Mater. Sci.*, 2020, **55**(32), 15367–15396.
216 Z. Xue, S. Wang, J. Yang, Y. Zhong, M. Qian, C. Li, Z. Zhang, G. Xing, S. Huettner, Y. Tao, Y. Li and W. Huang, *npj Flexible Electron.*, 2018, **2**(1), 1.
217 J. Li, L. Fang, B. Sun, X. Li and S. H. Kang, *J. Electrochem. Soc.*, 2020, **167**(3), 037561.
218 R. D. Pyarasani, T. Jayaramudu and A. John, *J. Mater. Sci.*, 2018, **54**(2), 974–996.
219 X. Yan, Q. Chen, Z. Huo, N. Zhang and M. Ma, *ACS Appl. Mater. Interfaces*, 2022, **14**(11), 13768–13777.
220 X. P. Hao, C. W. Zhang, X. N. Zhang, L. X. Hou, J. Hu, M. D. Dickey, Q. Zheng and Z. L. Wu, *Small*, 2022, **18**(23), e2201643.
221 J. Liu, H. Wang, R. Ou, X. Yi, T. Liu, Z. Liu and Q. Wang, *Chem. Eng. J.*, 2021, **426**, 130722.
222 Q. Li, L. N. Zhang, X. M. Tao and X. Ding, *Adv. Healthcare Mater.*, 2017, **6**(12), 1601371.
223 H. Ding, Z. Wu, H. Wang, Z. Zhou, Y. Wei, K. Tao, X. Xie and J. Wu, *Mater. Horiz.*, 2022, **9**(7), 1935–1946.
224 H. Zhou, Z. Wang, W. Zhao, X. Tong, X. Jin, X. Zhang, Y. Yu, H. Liu, Y. Ma, S. Li and W. Chen, *Chem. Eng. J.*, 2021, **403**, 126307.
225 F. Mo, Y. Huang, Q. Li, Z. Wang, R. Jiang, W. Gai and C. Zhi, *Adv. Funct. Mater.*, 2021, **31**(28), 2010830.
226 Y. Zhao, N. Yang, X. Chu, F. Sun, M. U. Ali, Y. Zhang, B. Yang, Y. Cai, M. Liu, N. Gasparini, J. Zheng, C. Zhang, C. F. Guo and H. Meng, *Adv. Mater.*, 2023, e2211617.
227 T. Yamada, Y. Hayamizu, Y. Yamamoto, Y. Yomogida, A. Izadi-Najafabadi, D. N. Futaba and K. Hata, *Nat. Nanotechnol.*, 2011, **6**(5), 296–301.
228 Y. Wang, T. Yang, J. Lao, R. Zhang, Y. Zhang, M. Zhu, X. Li, X. Zang, K. Wang, W. Yu, H. Jin, L. Wang and H. Zhu, *Nano Res.*, 2015, **8**(5), 1627–1636.
229 Y. Lu, Z. Liu, H. Yan, Q. Peng, R. Wang, M. E. Barkey, J. W. Jeon and E. K. Wujcik, *ACS Appl. Mater. Interfaces*, 2019, **11**(22), 20453–20464.
230 K. Ren, Y. Cheng, C. Huang, R. Chen, Z. Wang and J. Wei, *J. Mater. Chem. B*, 2019, **7**(37), 5704–5712.
231 D. Zhang, B. Ren, Y. Zhang, L. Xu, Q. Huang, Y. He, X. Li, J. Wu, J. Yang, Q. Chen, Y. Chang and J. Zheng, *J. Mater. Chem. B*, 2020, **8**(16), 3171–3191.
232 T. Wang, Y. Zhang, Q. Liu, W. Cheng, X. Wang, L. Pan, B. Xu and H. Xu, *Adv. Funct. Mater.*, 2018, **28**(7), 1705551.
233 L. Pan, A. Chortos, G. Yu, Y. Wang, S. Isaacson, R. Allen, Y. Shi, R. Dauskardt and Z. Bao, *Nat. Commun.*, 2014, **5**, 3002.
234 G. Min, Y. Xu, P. Cochran, N. Gadegaard, D. M. Mulvihill and R. Dahiya, *Nano Energy*, 2021, **83**, 105829.
235 Y. Xu, G. Min, N. Gadegaard, R. Dahiya and D. M. Mulvihill, *Nano Energy*, 2020, **76**, 105067.
236 G. Min, G. Khandelwal, A. S. Dahiya, D. Mulvihill and R. Dahiya, *IEEE J. Flexible Electron.*, 2022, DOI: **10.1109/JFLEX.2022.3225128**.
237 Z. Wu, H. Ding, K. Tao, Y. Wei, X. Gui, W. Shi, X. Xie and J. Wu, *ACS Appl. Mater. Interfaces*, 2021, **13**(18), 21854–21864.
238 H. Jeong, J. A. Rogers and S. Xu, *Sci. Adv.*, 2020, **6**(36), eabd4794.
239 Y. Zhao, C. Y. Lo, L. Ruan, C. H. Pi, C. Kim, Y. Alsaid, I. Frenkel, R. Rico, T. C. Tsao and X. He, *Sci. Rob.*, 2021, **6**(53), eabd5483.
240 L. Liu, S. Luo, Y. Qing, N. Yan, Y. Wu, X. Xie and F. Hu, *Macromol. Rapid Commun.*, 2018, **39**(10), e1700836.
241 J. Wu, Z. Wu, Y. Wei, H. Ding, W. Huang, X. Gui, W. Shi, Y. Shen, K. Tao and X. Xie, *ACS Appl. Mater. Interfaces*, 2020, **12**(16), 19069–19079.
242 S. Hao, L. Meng, Q. Fu, F. Xu and J. Yang, *Chem. Eng. J.*, 2022, **431**, 133782.
243 J. Wu, Z. Wu, S. Han, B. R. Yang, X. Gui, K. Tao, C. Liu, J. Miao and L. K. Norford, *ACS Appl. Mater. Interfaces*, 2019, **11**(2), 2364–2373.
244 Y. Wei, H. Wang, Q. Ding, Z. Wu, H. Zhang, K. Tao, X. Xie and J. Wu, *Mater. Horiz.*, 2022, **9**(7), 1921–1934.
245 Z. Wu, L. Rong, J. Yang, Y. Wei, K. Tao, Y. Zhou, B. R. Yang, X. Xie and J. Wu, *Small*, 2021, **17**(52), e2104997.
246 J. L. Puckett and S. C. George, *Respir. Physiol. Neurobiol.*, 2008, **163**(1–3), 166–177.
247 J. Zhou, X. F. Cheng, B. J. Gao, C. Yu, J. H. He, Q. F. Xu, H. Li, N. J. Li, D. Y. Chen and J. M. Lu, *Small*, 2019, **15**(2), e1803896.
248 Q. Ding, Z. Zhou, H. Wang, Z. Wu, K. Tao, B. R. Yang, X. Xie, J. Fu and J. Wu, *SmartMat*, 2022, **4**, 1.
249 Z. Ma, P. Chen, W. Cheng, K. Yan, L. Pan, Y. Shi and G. Yu, *Nano Lett.*, 2018, **18**(7), 4570–4575.
250 Y. Lin, Z. Wu, C. Li, Q. Ding, K. Tao, K. Zhai, M. Chen, M. Zilberman, X. Xie and J. Wu, *EcoMat*, 2022, **4**(6), e12220.
251 Y. Liang, Z. Wu, Y. Wei, Q. Ding, M. Zilberman, K. Tao, X. Xie and J. Wu, *Nanomicro Lett.*, 2022, **14**(1), 52.
252 V. P. Vu, L. H. Sinh and S. H. Choa, *ChemNanoMat*, 2020, **6**(11), 1522–1538.
253 Y. Liang, Q. Ding, H. Wang, Z. Wu, J. Li, Z. Li, K. Tao, X. Gui and J. Wu, *Nanomicro Lett.*, 2022, **14**(1), 183.
254 Q. Ding, H. Wang, Z. Zhou, Z. Wu, K. Tao, X. Gui, C. Liu, W. Shi and J. Wu, *SmartMat*, 2022, **4**(2), e1147.
255 E. S. Muckley, J. Lynch, R. Kumar, B. Sumpter and I. N. Ivanov, *Sens. Actuators, B*, 2016, **236**, 91–98.
256 X. Zhang, W. Yang, H. Zhang, M. Xie and X. Duan, *Nanotechnol. Precis. Eng.*, 2021, **4**(4), 045004.

257 Z. Xu, F. Zhou, H. Yan, G. Gao, H. Li, R. Li and T. Chen, *Nano Energy*, 2021, **90**, 106614.
258 Q. Zhang, X. Liu, L. Duan and G. Gao, *J. Mater. Chem. A*, 2020, **8**(8), 4515–4523.
259 Z. Xie, Z. Chen, X. Hu, H.-Y. Mi, J. Zou, H. Li, Y. Liu, Z. Zhang, Y. Shang and X. Jing, *J. Mater. Chem. C*, 2022, **10**(21), 8266–8277.
260 X. Liu, K. J. Gilmore, S. E. Moulton and G. G. Wallace, *J. Neural. Eng.*, 2009, **6**(6), 065002.
261 X. Pei, H. Zhang, Y. Zhou, L. Zhou and J. Fu, *Mater. Horiz.*, 2020, **7**(7), 1872–1882.
262 S. Liang, Y. Zhang, H. Wang, Z. Xu, J. Chen, R. Bao, B. Tan, Y. Cui, G. Fan, W. Wang, W. Wang and W. Liu, *Adv. Mater.*, 2018, **30**(23), e1704235.
263 D. Gao, K. Parida and P. S. Lee, *Adv. Funct. Mater.*, 2019, **30**(29), 1907184.
264 R. Green and M. R. Abidian, *Adv. Mater.*, 2015, **27**(46), 7620–7637.
265 M. R. Abidian, K. A. Ludwig, T. C. Marzullo, D. C. Martin and D. R. Kipke, *Adv. Mater.*, 2009, **21**(37), 3764–3770.
266 W. Zhang, P. Feng, J. Chen, Z. Sun and B. Zhao, *Prog. Polym. Sci.*, 2019, **88**, 220–240.
267 Y. Shi, L. Pan, B. Liu, Y. Wang, Y. Cui, Z. Bao and G. Yu, *J. Mater. Chem. A*, 2014, **2**(17), 6086–6091.
268 C. R. Chen, H. Qin, H. P. Cong and S. H. Yu, *Adv. Mater.*, 2019, **31**(19), e1900573.
269 Y. Liu, A. Gao, J. Hao, X. Li, J. Ling, F. Yi, Q. Li and D. Shu, *Chem. Eng. J.*, 2023, **452**, 139605.
270 W. Teng, Q. Zhou, X. Wang, H. Che, P. Hu, H. Li and J. Wang, *Chem. Eng. J.*, 2020, **390**, 124569.
271 H. Mi, X. Yang, F. Li, X. Zhuang, C. Chen, Y. Li and P. Zhang, *J. Power Sources*, 2019, **412**, 749–758.